

1 Dear Referee,

2 Thank you very much for your valuable suggestions and comments. We have tried to implement  
3 each point by point. Please see the blue coloured text is answers to the query. Detailed explanations  
4 with updated figures have been incorporated in the revised manuscript.

5 **Referee#2**

6

7 General comments:

8 This ambitious study considers a range of mechanisms affecting CO<sub>2</sub> and CH<sub>4</sub> concentrations  
9 over the course of a year. Given the range of mechanisms involved, the approach needs to be far  
10 more systematic and the analysis more robust. In many places, the discussion does not relate  
11 closely enough to the data – results are presented and then an explanation is suggested based on  
12 literature, without any testing or demonstration of its relevance to this dataset. It is often not clear  
13 to the reader why a particular plot or grouping of data has been chosen. As many of the findings  
14 are not clear-cut, this leads the reader to question whether the results are robust or whether the  
15 conclusions would be different if data had been analysed slightly differently. In some places, there  
16 seems to be a very large jump between the data presented and the conclusions drawn. One key  
17 issue is the relative importance of the various mechanisms considered. In each subsection (of  
18 Section 4) the mechanism under consideration is used to explain the results as presented in that  
19 subsection, while the other processes (some of which have been shown to be major controls) are  
20 generally ignored.

21 In terms of the methodology, important information is missing about the study area in particular.  
22 It is often unclear how data have been averaged and why. The paper needs restructuring so that the  
23 reader understands the aims, approach and decisions taken by the authors.

24 The manuscript also has several typographical errors and language issues (not all detailed here).

25 **Specific comments referring to particular lines are given below:**

26 **Introduction:**

27 The Introduction needs restructuring and developing. A clear outline of objectives is needed. A  
28 summary of the various mechanisms that will be examined in the rest of the paper would improve  
29 readability. Previous work that is relevant to this study should be discussed.

30 Pg. 34207 Line 12-5: It is not clear why this sentence appears here. It would fit more naturally in  
31 Section 3.2.2.

32 **Answer:** We have incorporated in section 3.2.2.

33 Pg. 34207 Line 16-23: This meaning of this paragraph is unclear.

34 **Answer:** Revised as suggested in the updated manuscript.

35 **Study area:**

36 More information about the study area is required. Figure 1a is not very informative and the scale  
37 is difficult to read. An aerial image, map or photograph of the study area would be far more helpful.  
38 What is the land use and land cover? Please provide some information about the characteristics of  
39 buildings and/or vegetation. Please provide some context for this study compared to other similar  
40 studies. How large is the study area?

41 [Answer: More details have been shown from figure 1a. The land use and land cover information](#)  
42 [added in the revised manuscript.](#)

43 Pg. 34208 Line 3: The site is described as ‘rural’ here but ‘suburban’ in the title.

44 [Answer: Corrected in the updated manuscript.](#)

45 Pg. 34208 Line 4: Population density would be more useful to facilitate comparison with other  
46 sites.

47 [Answer: Population density information provided in the revised manuscript.](#)

48 5). Pg. 34208 Line 9: What is meant by ‘near’? Please quantify.

49 [Answer: Updated in the revised manuscript.](#)

50 **Data set and methodology:**

51 Pg. 34208 Line 23-5: This paragraph does not communicate very much. It may be more  
52 informative to provide a brief summary of which variables are being measured or modelled and  
53 why here, before moving on to the subsections giving the details of each. Currently, the reader  
54 does not have a clear overview of the campaign.

55 [Answer: We already presented in table.1.](#)

56 ***In-situ observations:***

57 More details are required about the experimental setup. Where are the sensors located (in terms of  
58 their surroundings and measurement height)?

59 [Answer: Updated in the revised manuscript.](#)

60 It is not clear how the data have been averaged. What is meant by ‘diurnally averaged’ (Pg. 34209  
61 Line 19)? What temporal resolution was used in Fig 2? In Fig 2a-b are these monthly averages and  
62 variation of daily values or hourly values or something else? What about in Fig 2c-d? What do the  
63 error bars represent?

64 In general, more detail is needed in the figure captions.

65 [Answer: Hourly data have been averaged. Fig 2a-b is updated as daily, weekly and monthly](#)  
66 [averages in the revised manuscript as reviewer suggested. Fig 2c-d updated as Fig 5a-d with](#)  
67 [additional boundary layer information as per referee suggestion. In the revised manuscript, Fig2c-](#)  
68 [d is monthly variation of GHGs against NDVI.](#)

69 In Fig 1b-e are the data monthly averages? Indicate the data are for 2014.

70 Answer: Yes monthly, updated in the manuscript.

71 Please also put y-axis ticks at more intuitive intervals on all plots (e.g. 50, 60, 70, and 80% in Fig  
72 1d).”

73 Answer: Corrected as suggested.

74 In Fig 3 and 4 what does each point represent? How have the data been averaged?

75 Answer: Daily average. In the current manuscript, figures have been updated with new numbering  
76 as per referee suggestion.

77 **Results and discussion** – the presentation and analysis of results needs significant improvement  
78 throughout this section. The discussion is often unclear and does not fully address the trends seen  
79 in the results. The explanations are often vague and, although processes are mentioned, they are  
80 not convincingly linked to the results of this study. The references used should be expanded here  
81 if relevant to this dataset, or used in the Introduction if they are useful as background instead.

82 Answer: More explanation with new references have been updated in the revised manuscript.

83 **Seasonal variations:**

84 12). Monthly averages are presented in Fig 2a-b but results are discussed in terms of seasons  
85 (consisting of 2, 3 or 4 months according to Section 2). Note it may be helpful to indicate the  
86 different seasons on Fig 2a-b.

87 Answer: Section 4.1 is updated with more explanation and new figure.

88 13). For CO<sub>2</sub>, the seasonal averages are very similar to each other, so it does not make sense to  
89 provide seasonal values and then talk about differences between behaviour in each season. Fig 2a  
90 suggests there may be relatively high CO<sub>2</sub> near the start of the monsoon season, although the period  
91 of missing data and considerable variability means the picture is not especially clear. If 1-week or  
92 2-week averages were used in Fig 2a instead, is the overall result the same? If the data are grouped  
93 according to the actual onset of the monsoon (rather than monthly approximations), are the results  
94 any more conclusive? The discussion and explanation (Pg. 34212 Line 4-13) does not give a clear  
95 overview of the processes involved, how they impact the CO<sub>2</sub> concentration and when or why  
96 each process is most significant.

97 Answer: With more explanation, section 4.1 is updated in the revised manuscript.

98 14). Pg. 34212 Line 4 ‘loss of carbon’ from what?

99 Answer: Less carbon budget in winter due to respiratory losses (Aurela et al. 2004). Updated in  
100 the revised manuscript.

101 15). For CH<sub>4</sub>, again, consideration should be given to the robustness and suitability of using  
102 monthly/seasonal averages. The analysis is vague and does not adequately explain the results. In  
103 particular, ‘associated with the Kharif season’ (Line 20) is vague and needs further explanation. Is  
104 the rate of change really highest during post-monsoon (OND) and winter (JF) (Line 26-7)? The

105 final sentence in Section 4.1 does not explain the results; please state and explain precisely what  
106 is meant (rather than 'This may be: : :').

107 [Answer: Present study analysis observed highest CH<sub>4</sub> concentration during post-monsoon and](#)  
108 [started decrease in subsequent seasons.](#)

109 **Diurnal variations:**

110 16). Pg. 34213 Line 5-7: The meaning of this sentence is unclear. Could you provide an example  
111 specific to this dataset?

112 [Answer: Sentence has been withdrawn and updated accordingly.](#)

113 17). Pg. 34213 Line 14-6: Referring to other studies is helpful, but are the sites in those studies  
114 similar, i.e. are the same processes relevant? More detailed discussion needed.

115 [Answer: Similar observations were made by Sharma et al. 2014 at Gadanki which has similar land](#)  
116 [use land cover as Shadnagar. Published results have been cited](#)

117 18). Pg. 34213 Line 16-20: Needs more explanation. Do boundary layer dynamics affect CH<sub>4</sub>  
118 concentrations as well? How does consideration of boundary layer height impact the findings from  
119 the previous subsection?

120 [Answer: Diurnal variations of atmospheric species such as CO<sub>2</sub> and CH<sub>4</sub> mainly controlled by](#)  
121 [boundary layer dynamics. However, the source and sink mechanisms for these gases may be](#)  
122 [different. More explanation provided at section 4.4 and 4.5.1 in the revised manuscript.](#)

123

124 **Influence of prevailing meteorology:**

125 19). Fig 3 – what does each point represent? Pg 34214 Line 2 mentions 'monthly mean wind  
126 speed'. Daily or hourly averages may be most suitable, bearing in mind the diurnal cycles seen in  
127 Fig 2.

128 [Answer: Daily averages](#)

129 20). Pg. 34214 Line 8-15: Wind direction and source area seem to be a very relevant consideration  
130 and should be addressed in more detail (again a map and some quantitative information would be  
131 useful).

132 [Answer: Land use land cover information given in Fig1 and quantitative information on influence](#)  
133 [of wind direction provided in table 3.](#)

134 21). Pg. 34214 Line 16 - Pg. 34215 Line 6: It is very difficult to relate the correlations discussed  
135 here to Figure 4, which leaves the reader rather unconvinced of the results. The analysis presented  
136 here does not seem sufficient to draw the conclusions reached in this section. Where other studies  
137 are used to try to explain potentially relevant processes, they are linked too vaguely to the results  
138 and there seems to be little evidence that these processes are actually relevant to the data shown  
139 here.

140 Answer: We tried to improve the quality of the figure for better visualization and interpretation.  
141 Meteorological processes which influence seasonal variations of GHGs has been provided in the  
142 updated manuscript.

143 22). Pg. 34214 Line 20: Is there any diurnal cycle in wind speed that should be accounted for? Do  
144 the findings change significantly if daily/hourly averages are used for wind  
145 speed/temperature/humidity?

146 Answer: These parameters (wind speed/temperature/humidity) will have diurnal behaviours as  
147 GHGs. We have not seen any significant between daily and hourly averages.

148 **Influence of boundary layer height on GHGs mixing ratios:**

149 23). the figure, discussion and conclusion do not give a clear picture of how the boundary layer  
150 height influences the mixing ratios.

151 Answer: X axis represents the seasonal transition i.e. monsoon to post monsoon (M-PM) etc. and  
152 y axis indicates seasonal difference of BLH and GHGs concentration respectively. We tried to  
153 bring out seasonal variation of BLH on GHGs using satellite and diurnal effect from ECMWF-  
154 ERA data sets.

155 **Methane sinks mechanism:**

156 24). Most of Section 4.5 would be better in the Introduction (which would also help the reader in  
157 Section 3 when the various datasets are described). Might the high CH<sub>4</sub> readings be due to the  
158 highway and railway directly? The dependence on OH seems like a hypothesis which can be  
159 neither supported nor rejected based on the analysis presented here.

160 Answer: For the continuity of manuscript, we updated section 4.5 as 4.6 in the revised manuscript.  
161 Yes, we observed high NO<sub>x</sub> values from the eastern direction (where highway and railways are  
162 there) which subsequently decreases OH radical through chemical process as described in the  
163 section 4.6. Due to which high values of CH<sub>4</sub> were observed during case study period.

164 **Influence of vegetation:**

165 25). Pg. 34218 Line 22-3: 'NDVI showed inverse relationship with CO<sub>2</sub>, mainly due to change in  
166 vegetation which affects the CO<sub>2</sub> concentrations.' Both halves of this sentence effectively say the  
167 same thing without explaining the process.

168 Answer: Typo error, sentence is reconstructed and updated in revised manuscript.

169 To summarise, Section 4 contains too many different mechanisms without consideration of how  
170 they impact each other or a clear systematic structure to the analysis. Perhaps the relationship with  
171 NDVI should be moved closer to the start of the section where seasonal variations are discussed.  
172 Looking at the monthly ratio (Fig 6) may also be more useful earlier on. The high CH<sub>4</sub> readings  
173 in Fig 7 may need to be discussed alongside source area analysis in Section 4.3.

174 Are there other sources or sinks of GHGs which have not been considered in this analysis? How  
175 might they impact the results?

176 [Answer: As per your suggestions, manuscript is rearranged and updated with more explanation.](#)

177 **Conclusions:**

178 26). the conclusion should draw together the findings and provide an insightful summary of the  
179 research. Many statements are vague (e.g. Pg 34221 Line 7-8: 'This clearly indicates the seasonal  
180 variations in source-sink mechanisms of CO<sub>2</sub> and CH<sub>4</sub> respectively.' What are the source-sink  
181 mechanisms and how do they differ for CO<sub>2</sub> and CH<sub>4</sub> with season?) What new findings have  
182 emerged from analysis of this dataset?

183 [Answer: As per your suggestions, manuscript is updated.](#)

184

185 **Minor comments:**

186 1). Throughout: Change GHG's to GHGs

187 [Answer: Updated in the revised manuscript.](#)

188 2). Pg 34206 Line 11-2: Sentence not clear – please rephrase.

189 [Answer: Rephrased as suggested](#)

190 3). Pg 34206 Line 16-7: Sentence vague and not clear– please rephrase.

191 [Answer: Updated in the revised manuscript.](#)

192 4). In many places spaces are missing, e.g. Pg. 34206 Line 22: '(GHG),particularly'; Pg. 34206  
193 Line 24: 'emissionsand'; Pg 34207 Line 8: 'andecosystems' ; Pg 34207 Line 9: 'reflector'

194 [Answer: Updated in the revised manuscript.](#)

195 5). Pg 34206 Line 26: What is the significance of May 2013? A longer-term perspective that  
196 extends to the present may be more useful (i.e. to indicate May 2013 is not an exception).

197 [Answer: This sentence has been modified in the revised manuscript.](#)

198 6). Pg 34209 Line 3: I would mention 'Los Gatos Research' here rather than in the Abstract and  
199 Introduction.

200 [Answer: Updated in the revised manuscript.](#)

201 7).Pg. 34209 Line 5-7: Reference would be useful here.

202 [Answer: Updated with Berman et al., 2012; Shea et al., 2013; Mahesh et al., 2015.](#)

203 8). Pg. 34209 Line 20-1: Give exact dates.

204 [Answer: We included exact dates in the revised manuscript.](#)

205 9). Pg. 34209 Line 25: Correct brackets.

206 [Answer: The correction is incorporated in the revised manuscript.](#)

207 10). Pg. 34211 Line 24: Better to define mean and standard deviation here rather than in the  
208 Abstract.

209 [Answer: This has been changed in the revised manuscript.](#)

210 11) Pg. 34212 Line 3-4: Change to ‘: : : ppm in winter, pre-monsoon, monsoon and postmonsoon,  
211 respectively’

212 [Answer: Updated in the revised manuscript.](#)

213 12). Pg. 34213 Line 22: Change ‘place’ to ‘plays’

214 [Answer: Updated in the revised manuscript.](#)

215

216

217

218

219

220

221

222

223

224

225

226

227

228

229

230

231

232

233

**Influence of Meteorology and interrelationship with greenhouse gases (CO<sub>2</sub> and CH<sub>4</sub>) at a sub-urban site of India**

Sreenivas. G, Mahesh. P\*, Subin Jose, Kanchana A. L., Rao P.V.N, Dadhwal. V.K

Atmospheric and Climate Sciences Group (ACSG),

Earth and Climate Science Area (ECSA),

National Remote Sensing Center (NRSC),

Indian Space Research Organization (ISRO),

Hyderabad, India-500037

\*Corresponding author: Mahesh P

Mail-Id:mahi952@gmail.com



## Abstract

Atmospheric greenhouse gases (GHGs), such as carbon dioxide (CO<sub>2</sub>) and methane (CH<sub>4</sub>), are important climate forcing agents due to their significant impacts on the climate system. The present study brings out first continuous measurements of atmospheric GHGs using high precision Los Gatos Research's greenhouse gas analyser (LGR-GGA) over Shadnagar, a suburban site of Central India during the period 2014. The annual mean of CO<sub>2</sub> and CH<sub>4</sub> over the study region are found to be 394±2.92 ppm and 1.92±0.07 ppm (mean (μ) ± 1std (σ)) respectively. CO<sub>2</sub> and CH<sub>4</sub> showed a significant seasonal variation during the study period with maximum (minimum) CO<sub>2</sub> observed during Pre-monsoon (Monsoon), while CH<sub>4</sub> recorded maximum during post-monsoon and minimum in monsoon. Irrespective of the seasons, consistent diurnal variations of a consistent diurnal mixing ratio of these gases are observed, with high (low) during night (afternoon) hours throughout the study period. Influences of prevailing meteorology (air temperature, wind speed, wind direction and relative humidity) on GHGs have also been investigated. CO<sub>2</sub> and CH<sub>4</sub> showed a strong positive correlation during winter, pre-monsoon, monsoon and post-monsoon with correlation coefficients (Rs) equal to 0.80, 0.80, 0.61 and 0.72 respectively, indicating common anthropogenic source for these gases. It implies the seasonal variations in source-sink mechanisms of CO<sub>2</sub> and CH<sub>4</sub>. Analysis of this study reveals the major sources for CO<sub>2</sub> are soil respiration and anthropogenic emissions while vegetation act as a main sink. Whereas the major source and sink for CH<sub>4</sub> are vegetation and presence of hydroxyl (OH) radicals.

Keywords: Carbon dioxide, Methane, OH radical.

Formatted: Subscript

Formatted: Subscript

## 1. Introduction

The Intergovernmental Panel on Climate Change (IPCC, 2013) reported that humankind is causing global warming through the emission of greenhouse gases (GHGs), particularly carbon dioxide (CO<sub>2</sub>) and methane (CH<sub>4</sub>). CO<sub>2</sub> and CH<sub>4</sub> concentrations have increased by 40% and 150 % respectively since pre-industrial times, mainly from fossil fuel emissions and secondarily from net land use change emissions (IPCC, 2013; Huang et al., 2015). CO<sub>2</sub> measurements at MaunaLoa, Hawaii (Monastersky, 2013) have exceeded the 400 ppm mark several times in May 2013. CH<sub>4</sub> is also receiving increasing attention due to high uncertainty in its sources and sinks (Keppler et al., 2006; Miller et al., 2007; Frankenberg et al., 2008). Stefanie Kirschke et al., (2013) reported that in India, agriculture and waste constitutes the single largest regional source of CH<sub>4</sub>. Although many sources and sinks have been identified for CH<sub>4</sub>, their relative contribution to atmospheric CH<sub>4</sub> is still uncertain (A. Garg et al., 2001; StefanieKirschke et al., 2013). In India, electric power generation ~~that~~ contributes to half of India's total CO<sub>2</sub> equivalent emissions (A. Garg et al., 2001).

Arid and semi-arid areas comprise about 30% of the Earth's land surface. Climate change and climate variability will likely have a significant impact on these regions (Huang et al., 2008; Huang et al., 2015). The variability of environmental factors may result in significant effects on regional climate and global climate (Wang et al., 2010), especially the radiative forcing: via the biogeochemical pathways affecting the terrestrial carbon cycle. Global climate change has serious impact on humans and ecosystems. Due to this, many factors have been identified that may reflect or cause variations in environmental change (Pielke et al., 2002). Out of these, the Normalized Difference Vegetation Index (NDVI) has become one of the most widely used indices to represent the biosphere influence on global change (Liu et al., 2011). ~~The planetary boundary layer (PBL) is the part of the atmosphere closest to the Earth's surface where turbulent processes often dominate the vertical redistribution of sensible heat, moisture, momentum, and aerosols/pollution (AO et al., 2012).~~

Greenhouse and other trace gases have great importance in atmospheric chemistry and for radiation budget of the atmosphere-biosphere system (Crutzen et al., 1991). Hydroxyl radicals (OH) are very reactive oxidizing agents, which are responsible for the oxidation of almost all gases that are emitted by natural and anthropogenic activities in the atmosphere. Atmospheric CO<sub>2</sub> measurements are very important for understanding the carbon cycle because CO<sub>2</sub> mixing ratios

in the atmosphere are strongly affected by photosynthesis, respiration, oxidation of organic matter, biomass and fossil fuel burning, and air–sea exchange process (Machida et al., 2003).

The present study brings out first continuous measurements of atmospheric GHG<sub>2</sub>s using high precision ~~Los Gatos Research's greenhouse gas analyser (LGR-GGA)~~ over Shadnagar, a suburban site of Central India during the period 2014. In addition to GHG<sub>2</sub>s observations, we have also made use of an automatic weather station (AWS) data along with model/satellite retrieved observation during the study period. Details about study area and data sets are described in the following sections.

## 2. Study Area

Shadnagar is situated in Mahabubnagar district of newly formed Indian state of Telangana. It is a ~~rural~~suburban location situated ~70km away from urban site of Hyderabad (Northern side) with a population of ~0.16 million (Patil et al., 2013). A schematic map of study area is shown in Fig. 1a. Major sources of pollutants over Shadnagar can be from small and medium scale industries, biomass burning and bio-fuel as well as from domestic cooking. In the present study sampling of GHG<sub>2</sub>s and related meteorological parameters are carried out in the premises of National Remote Sensing Center (NRSC), ~~Shadnagar~~, Shadnagar Campus (17°02'N, 78°11'E). Sampling site is near (aerial distance ~ 2.25 km) to National highway 7 (NH7) and a railway track (non-electrified) is in the East (E) direction.

Mean monthly variations of temperature (°C) and relative humidity (RH (%)) observed at Shadnagar during 2014 are shown in Figure 1e and 1d respectively. The Indian Meteorological Department (IMD) defined monsoon as June-July-August-September (JJAS), post-monsoon (October-November-December-OND), winter (January-February-JF) and pre-monsoon (March-April-May-MAM) in India. Temperature over Shadnagar varies from ~20°C to ~29°C. Relative humidity (RH) in Shadnagar reached a maximum of ~82 % in monsoon from a minimum of ~48 % recorded during pre-monsoon. Surface wind speed (Fig. 1c) varies between 1.3 to 1.6 m s<sup>-1</sup> with a maximum observed during monsoon and minimum in pre-monsoon. The air mass advecting (Fig. 1b) towards study site is either easterly or westerly. The easterly wind prevails during winter and gradually shifts to south-westerlies in pre-monsoon, and dominates during monsoon.

## 3. Data set and Methodology

Details about the instrument and data utilized are discussed in this section. The availability and frequency of the observations all data used in present study are tabulated in Table 1.

### 3.1 In-situ observations

#### 3.1.1 Greenhouse Gas Analyser (GGA)

The Los Gatos Research's - Greenhouse Gas Analyser (model: LGR-GGA-24EP) is an advanced instrument capable of simultaneous measurements of CO<sub>2</sub>, CH<sub>4</sub> and H<sub>2</sub>O. This instrument is well known for high precision and accuracy which are crucial towards understanding background concentrations of atmospheric GHGs, with specifications meeting WMO standards of measurement (Berman et al., 2012; Shea et al., 2013; Mahesh et al., 2015). It is based on enhanced Off-Axis Integrated Cavity Output Spectroscopy (OA-ICOS) technology (Paul et al. 2001, Baer et al., 2002), which utilizes true wavelength scanning to record fully resolved absorption line shapes. Considering the rural nature of the site, flow rate is fixed to be 7 liters per minute (lpm). Ambient air entering the GGA is analysed using two near infrared (NIR) distributed feedback tunable diode lasers (TDL), one for a CO<sub>2</sub> absorption line near 1.60  $\mu\text{m}$  ( $\nu_0 = 6250\text{ cm}^{-1}$ ) and the other to probe CH<sub>4</sub> and H<sub>2</sub>O absorption lines near 1.65  $\mu\text{m}$  ( $\nu_0 = 6060.60\text{ cm}^{-1}$ ). The concentration of the gases is determined by the absorption of their respective characteristic absorption lines with a high sampling time of 1sec. A detailed explanation regarding the configuration, working and calibration procedure performed for GGA in NRSC can be found elsewhere in Mahesh et al., (2015). In the present study we used GGA retrieved CO<sub>2</sub> and CH<sub>4</sub> data. High resolution data sets are diurnally averaged and is used in further analysis. Due to failure of internal central processing unit (CPU) of the analyzer, data are not recorded from pre-monsoon month of 1<sup>st</sup> May to a few days in 18<sup>th</sup> June during the study period.

#### 3.1.2 O<sub>3</sub> and NO<sub>x</sub> analyzer

Surface concentrations of O<sub>3</sub> and NO<sub>x</sub> have been measured continuously using on-line analyzers (Model No.s: 49i and 42i for O<sub>3</sub> and NO<sub>x</sub> respectively), procured from Thermo Scientific, USA since July 2014. The trace gases (O<sub>3</sub> and NO<sub>x</sub>) sampling inlet is installed on the top of a 2 m mast fixed on the roof of an 8 m high building, and ambient air flow is supplied to the instruments. The inlet prevents the ingress of rain water, and is equipped with 0.5  $\mu\text{m}$  filter to prevent accumulation of dust within the instrument. The ozone analyzer is based on Beer-Lambert-

Formatted: Superscript

Formatted: Superscript

Formatted: Subscript

Formatted: Subscript

Baugher law which relates absorption of light to the concentration of species as its operating principle and has an in-built calibration unit for conducting periodical span and zero checks. The NO<sub>x</sub> analyzer utilizes a molybdenum converter to convert NO<sub>2</sub> into NO and estimates the NO<sub>x</sub> concentration by the intensity of light emitted during the chemiluminescent reaction of NO with O<sub>3</sub> present in the ambient air. The analyzer is integrated with zero and span calibrations which are performed twice monthly.

Simultaneous observations of meteorological parameters are obtained from an automatic weather station (AWS) ~~located in the same campus, installed in NRSC, Shadnagar campus as a part of Calibration and Validation (CAL/VAL) project in March 2012 is equipped with nine sensors to measure fifteen weather parameters. Weather parameters measured are at surface level and height of the AWS mast is ~10 meters. Wind speed and direction measurements are collected at the maximum height (3m) and all others are at 1-1.5m height.~~

Formatted: Line spacing: 1.5 lines

Formatted: Strikethrough

### 3.2 Satellite and Model observations

#### 3.2.1 MODIS

Moderate-resolution Imaging Spectrometer (MODIS) is launched in December 1999 on the polar-orbiting NASA-EOS Terra platform (Salomonson et al. 1989; King et al. 1992). It has 36 spectral channels and acquires data in 3 spatial resolutions of 250 m, 500 m, and 1 km (channels 8–36), covering the visible, near-infrared, shortwave infrared, and thermal-infrared bands. In the present study we used monthly Normalised Difference Vegetation Index (NDVI) data obtained from Terra/MODIS at 5 km spatial resolution. The NDVI value is defined as following ratio of albedos ( $\alpha$ ) at different wavelengths:

$$NDVI = \frac{\alpha_{0.86\mu m} + \alpha_{0.67\mu m}}{\alpha_{0.86\mu m} - \alpha_{0.67\mu m}} \quad (1)$$

NDVI values can range from -1.0 to 1.0 but typical ranges are from 0.1 to 0.7, with higher values associated with greater density and greenness of plant canopies. More details of the processing methods used in generating the data set can be found in James and Kalluri (1994).

#### 3.2.2 COSMIS-RO

COSMIC (Constellation Observation System for Meteorology, Ionosphere and Climate) is a GPS (Global Positioning System) radio occultation (RO) observation system (Wang et al., 2013).

It consists of six identical microsatellites, and was launched successfully on 14 April 2006. GPS radio occultation observation has the advantage of near-global coverage, all-weather capability, high vertical resolution, high accuracy and self-calibration (Yunck et al., 2000). Geophysical parameters ~~(such as, temperature and humidity profiles)~~like temperature and humidity profiles have been simultaneously obtained from refractivity data using one-dimensional variational (1DVAR) analysis. Further COSMIC-RO profiles are used to estimate planetary boundary layer height (BLH). BLH is defined to be the height at which the vertical gradient of the refractivity or water vapor partial pressure is minimum (Ao et al., 2012), explained detail methodology for calculating the BLH from refractivity (N). The planetary boundary layer (PBL) is part of the atmosphere closest to the Earth's surface where turbulent processes often dominate the vertical redistribution of sensible heat, moisture, momentum, and aerosols/pollution (AO et al., 2012).

### 3.2.3 Hysplit model

The general air mass pathway reaching over Shadnagar is analysed using HYSPLIT model (Draxler and Rolph, 2003) [http://www.arl.noaa.gov/ready/hysplit4.html]. We computed 5 day isentropic model backward air mass trajectory for all study days with each trajectory starting at 00:00 UTC and reaching study site, (Shadnagar) at different altitudes (1 km, 2 km, 3 km and 4 km). Even though the trajectory analysis have inherent uncertainties (Stohl, 1998), they are quite useful in determining long range circulation.

## 4. Results and Discussion

### 4.1 Seasonal variations of CO<sub>2</sub> and CH<sub>4</sub>

~~Temporal~~Monthly variations of CO<sub>2</sub> and CH<sub>4</sub> during the study period are shown in Figure. 2a and 2b. The circles indicate the daily mean, while triangular markers represent weekly averages and monthly mean by square markers. Annual mean of CO<sub>2</sub> over study region is found to be  $394 \pm 2.92$  ~~(mean ( $\mu$ )  $\pm$  standard deviation ( $1\sigma$ ))~~( $\mu \pm 1\sigma$ ) ppm with an observed minimum in monsoon and maximum in pre-monsoon. ~~Seasonal mean~~Background (average) values of CO<sub>2</sub> observed during different seasons are  $393 \pm 5.60$ ,  $398 \pm 7.60$ , ~~and~~  $392 \pm 7.0$ , and  $393 \pm 7.0$  ppm ~~in with~~respectively winter, pre-monsoon, monsoon, and post-monsoon respectively. Minimum CO<sub>2</sub> during winter (dry season) ~~can be due to respiratory~~indicates the loss of carbon (Gilmanov et al., 2004; Aurela et al. 2004) as decreased temperature and solar radiation during this period inhibit increases in local CO<sub>2</sub> assimilation (Thum et al., 2009). A steady increase in CO<sub>2</sub> concentration is

observed as season changes from winter to pre-monsoon months. Enhancement in Pre-monsoon is due to higher temperature and solar radiation prevailing during these months which stimulate the assimilation of CO<sub>2</sub> in the daytime and respiration in the night (Fang et al., 2014). The enhanced soil respiration during these months also compliments the increase in CO<sub>2</sub> concentration during this period. In addition to these natural causes, biomass burning over Indian region can also have a significant effect on pre-monsoon CO<sub>2</sub> concentration. More detailed explanation of biomass burning influence on pre-monsoon GHGs concentration is discussed in section 4.6.- Surface CO<sub>2</sub> concentration recorded a minimum during monsoon months can be mainly because of enhanced photosynthesis processes with the availability of greater soil moisture. A decrease in CO<sub>2</sub> concentration is also observed as the monsoon progress. The decreases in temperature (due to cloudy and overcast conditions prevailing during these months) reduce leaf and soil respiration which contributes to the enhancement of carbon uptake (Patil et al., 2013; Jing et al., 2010). Further increase during post-monsoon CO<sub>2</sub> is associated with high ecosystem productivity (Sharma et al., 2014) also an enhancement in soil microbial activity (Stefanie Kirschke et al., 2013).

CH<sub>4</sub> concentration in the troposphere is principally determined by a balance between surface emission and destruction by hydroxyl radicals (OH). The major sources for CH<sub>4</sub> in the Indian region are rice, paddies, wetlands and ruminants (Schneising et al., 2009). Annual CH<sub>4</sub> concentration over study area is observed to be  $1.92 \pm 0.07$  ppm, with a maximum ( $2.02 \pm 0.01$  ppm) observed in post-monsoon and minimum ( $1.85 \pm 0.03$  ppm) in monsoon. Seasonal mean (average) values of CH<sub>4</sub> observed during different seasons are  $1.93 \pm 0.05$ ,  $1.89 \pm 0.05$ ,  $1.85 \pm 0.03$ , and  $2.02 \pm 7$  ppm with respectively winter, pre-monsoon, monsoon, and post-monsoon. The highest concentration appears during post-monsoon and may be associated with the Kharif season (Goroshiet al., 2011). Seasonal meanBackground (average) values of CH<sub>4</sub> observed during different seasons are  $1.93 \pm 0.05$ ,  $1.89 \pm 0.05$ , and  $1.85 \pm 0.03$ , and  $2.02 \pm 7$  ppm with respectively winter, pre-monsoon, monsoon, and post-monsoon. Hayashida et al. (2013) reported that The seasonality of CH<sub>4</sub> concentration over monsoon Asia is characterized by higher values in the wet season and lower values in the dry season; possibly because of the effects of strong emissions from rice paddies and wetlands during the wet season. Low mixing ratios of CH<sub>4</sub> observed during monsoon season were mainly due to the reduction in atmospheric hydrocarbons because of the reduced photochemical reactions and the substantial reduction in solar intensity (Abhishek Gaur et al 2014).The rate of change of CH<sub>4</sub> was found to be high during post-monsoon, and winter. Both

biological and physical processes control the exchange of CH<sub>4</sub> between rice paddy fields and the atmosphere (Nishanth et al., 2014; Goroshiet al., 2011). Due to this, This may be one of the major reasons for the enhanced CH<sub>4</sub> observed during post-monsoon at present study area and winter seasons (Nishanth et al., 2014; Sheshakumar et al., 2011).

#### 4.2 Influence of vegetation on GHGs.

In India cropping season is classified into (i) Kharif and (ii) Rabi based on the onset of monsoon. The Kharif season is from July to October during the south-west (SW) monsoon and Rabi season is from October to March (Koshal Avadhesh, 2013). NDVI being one of the indicators of vegetation change, monthly variations of CO<sub>2</sub> and CH<sub>4</sub> against NDVI is studied to understand the impact of land use land cover on mixing ratios of CO<sub>2</sub> and CH<sub>4</sub>. Monthly mean changes in NDVI, CO<sub>2</sub> and CH<sub>4</sub> are shown in Figure 2c and 2d. Monthly mean of GHGs represented in this analysis is calculated from daily mean in day time (10-16 LT). Analysis of the figure reveals that an inverse relationship exists between NDVI and CO<sub>2</sub>; while a positive relation is observed w.r.t CH<sub>4</sub>. Generally over this part of the country vegetation starts during the month of June with the onset of SW monsoon and as vegetation increases a decrease in CO<sub>2</sub> concentration is observed, due to enhancement in photosynthesis. Further a decline in NDVI is observed as the season advances from post monsoon to winter and then to pre-monsoon, and it is associated with an increase in CO<sub>2</sub> concentration. Similarly, the main source for CH<sub>4</sub> emissions are soil microbial (Stefanie Kirschke et al., 2013) activity which are more active during monsoon and post monsoon seasons. High (low) soil moisture and NDVI is observed in monsoon (pre monsoon) seasons (Figure 8a and 8b). The predominating factors which controls the soil emissions of CO<sub>2</sub>, CH<sub>4</sub> are moisture content, soil temperature, vegetation and soil respiration (Smith et al., 2003; Jones et al., 2005; Chen et al., 2010) respectively.

Biomass burning (forest fire and crop residue burning) is one of the major sources of gaseous pollutants such as carbon monoxide (CO), methane (CH<sub>4</sub>), nitrous oxides (NO<sub>x</sub>) and hydrocarbons in the troposphere (Crutzen et al., 1990, 1985; Sharma et al., 2010). In order to study the role of biomass burning on GHGs a case study is discussed. Figure 43c shows the spatial distribution of MODIS derived fire counts over Indian region during 14-21 April 2014 with air mass trajectories ending over study area over layed on it at different altitudes viz. 1000 m, 2000 m and 4000 m respectively. Analysis of the figure shows a number of potential fire

Formatted: Subscript

Formatted: Subscript



locations on the north-western and south-eastern side of study location and trajectories indicate its possible transport to study area. Daily mean variation of GHGs during the month of April 2014 (Figure 43b) indicates an enhancement in GHGs during the same period (14-21 April 2014). Analysis reveals that CO<sub>2</sub> and CH<sub>4</sub> have increased by ~2% and ~0.06% respectively during event days with respect to monthly mean. This analysis reveals that long range / regional transported biomass burning have a role in enhancement of GHGs over study site. Further to understand the seasonal variation of biomass burning contribution to GHGs we analysed long term (2003-2013) Fire Energetics and Emissions Research version 1.0 (FEER v1) data over study area. Emission coefficient (C<sub>e</sub>) products during biomass burning is developed from coincident measurements of fire radiative power (FRP) and AOD from MODIS Aqua and Terra satellites (Ichoku and Ellison, 2014). Figure 43a shows seasonal variation of CO<sub>2</sub> emission due to biomass burning over the study site. Enhancement in CO<sub>2</sub> emission is seen during pre-monsoon months; which also supports earlier observation (Figure 2a). This analysis reveals that biomass burning has a role in pre-monsoon enhancement of CO<sub>2</sub> over study site. For a qualitative analysis of this long range transport, we have analysed air mass trajectories ending over study site during different seasons.

#### **4.3 Correlation between CO<sub>2</sub> and CH<sub>4</sub>**

A correlation study is carried out between hourly averaged CO<sub>2</sub> and CH<sub>4</sub> during all season for the entire study period. The statistical analysis for different seasons is shown in Table 32. Fang et al., (2015) suggest the correlation coefficients (Rs) value higher than 0.50 indicates a similar source mechanism of CO<sub>2</sub> and CH<sub>4</sub>. Also a positive correlation dominance of anthropogenic emission on carbon cycle. Our study also reveals a strong positive correlation observed between CO<sub>2</sub> and CH<sub>4</sub> during winter, pre-monsoon, monsoon, and post-monsoon with R equal to 0.80, 0.80, 0.61, and 0.72 respectively. Seasonal regression coefficients (slope) and their uncertainties ( $\psi_{\text{slope}}$ ,  $\psi_{\text{y-int}}$ ) are computed using Taylor (1997) which showed maximum during winter, pre-monsoon, and minimum in a monsoon that figure out the hourly stability of the mixing ratios between CO<sub>2</sub> and CH<sub>4</sub>. This can be due to relatively simple source/sink process of CO<sub>2</sub> in comparison with CH<sub>4</sub>. Figure 54 shows the seasonal variation of  $\Delta\text{CH}_4/\Delta\text{CO}_2$ . Dilution effects during transport of CH<sub>4</sub> and CO<sub>2</sub> can be minimized to some extent by dividing the increase of CH<sub>4</sub> over time by the respective increase in CO<sub>2</sub> (Worthy et al., 2009). In this study, background concentrations of

respective GHGs are determined as mean values of the 1.25 percentile of data for monsoon, post-monsoon, pre-monsoon and winter (Pan et al., 2011; Worthy et al., 2009). Annual  $\Delta\text{CH}_4/\Delta\text{CO}_2$  over the study region during the study period is found to be 7.1 (ppb/ppm). This low value clearly indicates the dominance of  $\text{CO}_2$  over the study region. The reported  $\Delta\text{CH}_4/\Delta\text{CO}_2$  values from some of the rural sites viz Canadian Arctic and Hateruma Island (China) are of the order 12.2 and ~10 ppb/ppm respectively (Worthy et al., 2009; Tohjima et al., 2014). Average  $\Delta\text{CH}_4/\Delta\text{CO}_2$  ratio during winter, pre-monsoon, monsoon and post-monsoon are 9.40, 6.40, 4.40, and 8.20 ppb respectively. Monthly average, of  $\Delta\text{CH}_4/\Delta\text{CO}_2$ , is relatively high from late post-monsoon to winter, when the biotic activity is relatively dormant (Tohjima et al., 2014). During pre-monsoon decrease in  $\Delta\text{CH}_4/\Delta\text{CO}_2$  ratio indicates the enhancement of  $\text{CO}_2$  relative to that of  $\text{CH}_4$ .

#### 4.2.4.4 Diurnal variations of $\text{CO}_2$ and $\text{CH}_4$

Figure 25ea to 5d and 2d shows the seasonally averaged diurnal cycle of  $\text{CO}_2$  and  $\text{CH}_4$  over Shadnagar during study period. The vertically bar represents the standard deviation from respective mean. Irrespective of seasonal variation GHGs showed a similar diurnal variation, with maximum mixing ratios observed during early morning (06:00 hrs) as well as early night hours (20:00 hrs) and minimum during afternoon hours. Figure 2e and 2d depicts seasonal diurnal variations of  $\text{CO}_2$  and  $\text{CH}_4$  over Shadnagar during study period. The amplitudes diurnal changes during seasonal variation mainly depend on biosphere sources and sinks such as land use and land cover change (Fearnside 2000, IPCC, and AR5). Maximum mixing ratios of  $\text{CO}_2$  and  $\text{CH}_4$  are observed during early morning and late night hours. Peak surface concentrations of  $\text{CO}_2$  and  $\text{CH}_4$  increase at night and remain high until sunrise (22:00hrs to 06:00hrs). However the difference observed in the maximum diurnal amplitudes can be attributed to seasonal changes. The observed diurnal cycle of GHGs is closely associated with diurnal variation of planetary boundary layer height (PBLH). For better understanding of the diurnal behavior of  $\text{CO}_2/\text{CH}_4$ , we used European Centre for Medium-range Weather Forecasting (ECMWF) Interim Reanalysis (ERA) PBL data set which gives the data for every three hours viz. 00:00, 03:00, 06:00, 09:00, 12:00, 15:00, 18:00, and 21:00 UTC with a resolution of  $0.25^\circ \times 0.25^\circ$  (<http://data-portal.ecmwf.int>). Figure 5a to 5d portrays the diurnal evolution of  $\text{CO}_2/\text{CH}_4$  during different season along with the evolution of Boundary Layer Height (m) on secondary y axis. The morning peak arises due to combined

Formatted: Subscript

Formatted: Subscript

Formatted: Subscript

Formatted: Subscript

influence of fumigation effect, (Stull 1988) and morning build-up of local anthropogenic activities (household and vehicular transport). Low value of GHGs as the day progress can be attributed to increased photosynthetic activity during day time and destruction of stable boundary layer and residual layer due convective activity. In the evening hours, surface inversion begins and form a shallow stable boundary layer (Nair et al., 2007) causing the enhancement in GHGs concentration near the surface. Figure 2e shows mixing ratios of CO<sub>2</sub> are gradually decreasing after sun rise and reaching peak minimum in the afternoon because of the net ecosystem uptake of the biosphere and boundary layer dynamics. During night time, mixing ratios increase due to formation of stable atmospheric boundary layer, soil respiration of the biosphere and absence of photosynthetic activity. Similar trend in diurnal variation of GHG's is reported from other parts of the country (Patil et al., 2013; Mahesh et al., 2014; Sharma et al., 2014; Nishanth et al., 2014). Although diurnal variations of CH<sub>4</sub> showed similar trend as of CO<sub>2</sub>, but are caused due to different factors. Lower troposphere acts as main sink for CH<sub>4</sub> with the formation of O<sub>3</sub> through oxidation of CH<sub>4</sub> and other trace species in the presence of NO<sub>x</sub> and hydroxyl radicals (OH) (Eisele et al., 1997, IPCC, AR5).

#### 4.3.4.5 Influence of prevailing meteorology

Redistribution (both horizontal and vertical) of GHG's also plays a role in their seasonal variation, as it controls transport and diffusion of pollutants from one place to another (Hassan 2015). A good inverse correlation between wind speed and GHG's suggest the proximity of sources near measurement site, while a not so significant correlation suggests the influence of regional transport (Ramachandran and Rajesh, 2007). Figure 3a and 3b shows scatter plot between GHG's and wind speed during different seasons. Analysis of Figure 3 shows that there exists an inverse correlation between daily mean wind speed and GHG's. Correlation coefficients (R<sub>s</sub>) between wind speed and CO<sub>2</sub> during pre-monsoon, monsoon, post-monsoon, and winter is 0.56, 0.32, 0.06, and 0.67 respectively. While for CH<sub>4</sub> it is found be 0.28, 0.71, 0.21, and 0.60 respectively. Negative correlation indicates that the influence of local sources on GHG's, however, poor correlation coefficients during different seasons suggest the role of regional/local transport (Mahesh et al 2014). Also an understanding of prevailing wind direction and its relationship with GHG's helps in determining their probable source regions. Table 23 shows the monthly mean variation of CO<sub>2</sub> and CH<sub>4</sub> with respect to different wind direction. Enhancement in CO<sub>2</sub> and CH<sub>4</sub> level over Shadnagar are observed to mainly come from NW and NE while the

lowest is from the S and SW. This can be associated to some extent with industrial emissions located in western side of sampling site, and the influence of emission and transport from nearby urban center on the NW side of the study site.

The influence of meteorological parameters (temperature and relative humidity) influence on trace gases is also examined. Figure 47a and 7b (top panel corresponds to CO<sub>2</sub> and bottom panel represents CH<sub>4</sub>) shows the scatter plot of temperature versus relative humidity as a function of GHGs during different seasons. Here, daily mean data is used instead of hourly mean data, to avoid the influence of the diurnal variations on correlations. CO<sub>2</sub> showed a positive correlation with temperature during all season except during winter. This negative correlation can be attributed to different response of photosynthesis rate to different air temperature decrease in rate of photosynthesis. IPCC (1990) reports that many mid-latitude plants shows an optimum gross photosynthesis rate when temperature varied from of 20 to 35 °C. The rate of plant respiration tends to be slow below 20°C. However, at higher temperatures, the respiration rate accelerates rapidly up to a temperature at which, it equals the rate of gross photosynthesis and there can be no net assimilation of carbon. While CH<sub>4</sub> showed a weak positive correlation with temperature during pre-monsoon and post-monsoon, while a weak negative correlation is observed during monsoon and winter. This could be due to the rate of chemical loss reaction with OH is faster in summer and minimum in other seasons. A case study on CH<sub>4</sub> sink mechanism has discussed in section 4.6. This indicates that regional air temperature doesn't significantly influence seasonal variation of CH<sub>4</sub> (Chen et al., 2015). Seasonal variation of GHG's also showed an insignificantly negative correlation with relative humidity. A similar observation is also reported by Abhishek et al., (2014). One of the supporting argument can be in humid conditions, these stoma can fully open to increase the uptake of CO<sub>2</sub> without a net water loss. Also, wetter soils can promote decomposition of dead plant materials, releasing natural fertilizers that help plants grow (Abhishek et al., 2014).

Figure 8a and 8b illustrates the daily mean variation of GHGs with respect to soil moisture and soil temperature (Top panel represent the seasonal variation of CO<sub>2</sub> w.r.t soil moisture and soil temperature, while bottom panel represent the seasonal variation of CH<sub>4</sub> against the same parameters with the same). It's quite interesting to observe that GHGs behave differently w.r.t soil moisture during different seasons. CH<sub>4</sub> shows a positive relationship during monsoon and post-monsoon and an inverse relationship exist during pre-monsoon and winter; while a reverse

Formatted: Subscript

relationship exist for CO<sub>2</sub>. During wet season aeration is restricted (Smith et al. 2003) hence soil respiration is limited, which decrease CO<sub>2</sub> flux. This can be one of the factors for low values of CO<sub>2</sub> during monsoon months, during dry months soil may act as sink of CH<sub>4</sub>.

#### **4.3.14.5.1 Influence of boundary layer height on GHGs mixing ratios**

The planetary boundary layer is the lowest layer of the troposphere where wind speed as a function of temperature plays major role in its thickness variation. It is an important parameter for controlling the observed diurnal variations and potentially masking the emissions signal (Newman et al., 2013). Since complete set of COSMIC RO data is not available during the study period, in this analysis we have analysed RO data from July 2013 to June 2014, along with simultaneous observations of GHG's. Monthly variations (Figure not show) of BLH computed from high vertical resolution of COSMIC-RO data against CO<sub>2</sub> and CH<sub>4</sub> concentrations. Monthly BLH is observed to be minimum (maximum) during winter and monsoon (pre monsoon) seasons and it closely resembles with the air temperature pattern. The highest (lowest) BLH over study region was identified 3.20 km (1.50 km). A monthly average monthly air temperature is maximum (minimum) of 29°C (20°C) during the summer (winter) months.

Seasonal BLH during winter, pre-monsoon, monsoon and post monsoon are 2.10 km, 3.15 km, 1.74 km and 2.30 km respectively. change in BLH thickness over study region was observed to be as Monsoon (M, 1.74 km) < winter (W, 2.10 km) < Post Monsoon (PM, 2.30 km) < Pre-monsoon (Pre-M, 3.15 km); its influence on CO<sub>2</sub> and CH<sub>4</sub> mixing ratios are shown in Figure 59a and 59b. X axis represents the seasonal transition i.e. monsoon to post monsoon (M-PM) etc and y axis indicates seasonal difference of BLH and GHGs concentration respectively. As seasonal BLH thickness increase, mixing ratios of CO<sub>2</sub> (CH<sub>4</sub>) decreased from 8.68 ppm to 5.86 ppm (110 ppb to 40 ppb). This effect clearly captured by seasonal diurnal averaged BLH data sets used from ECMWF-ERA. The amount of biosphere emissions influence on CO<sub>2</sub> and CH<sub>4</sub> can be estimated through atmospheric boundary layer processes. Since the study region being a flat terrain, variations in CO<sub>2</sub> and CH<sub>4</sub> were mostly influenced by boundary layer BLH thickness through convection and biosphere activities.

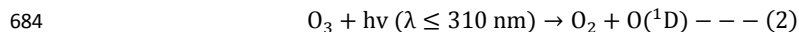
#### **4.4 Correlation between CO<sub>2</sub> and CH<sub>4</sub>**

A correlation study is carried out between hourly averaged CO<sub>2</sub> and CH<sub>4</sub> during all season for the entire study period. The statistical analysis for different seasons is shown in Table 3. Fang et al., (2015) suggest the correlation coefficient (R) value higher than 0.50 indicates a similar source mechanism of CO<sub>2</sub> and CH<sub>4</sub>. Also a positive correlation dominance of anthropogenic emission on carbon cycle. Our study also reveals a strong positive correlation observed between CO<sub>2</sub> and CH<sub>4</sub> during winter, pre-monsoon, monsoon and post-monsoon with R equal to 0.80, 0.80, 0.61 and 0.72 respectively. Seasonal regression coefficients (slope) and their uncertainties ( $\psi_{\text{slope}}$ ,  $\psi_{y\text{-int}}$ ) are computed using Taylor (1997) which showed maximum during winter, pre-monsoon and minimum in a monsoon that figure out the hourly stability of the mixing ratios between CO<sub>2</sub> and CH<sub>4</sub>. This can be due to relatively simple source/sink process of CO<sub>2</sub> in comparison with CH<sub>4</sub>. Dilution effects during transport of CH<sub>4</sub> and CO<sub>2</sub> can be minimized to some extent by dividing the increase of CH<sub>4</sub> over time by the respective increase in CO<sub>2</sub> (Worthy et al., 2009). Figure 6 shows the seasonal variation of  $\Delta\text{CH}_4/\Delta\text{CO}_2$ . In this study, background concentrations of respective GHG's are determined as mean values of the 1.25 percentile of data for monsoon, post-monsoon, pre-monsoon and winter (Pan et al., 2011; Worthy et al., 2009). Annual  $\Delta\text{CH}_4/\Delta\text{CO}_2$  over the study region during the study period is found to be 7.1 (ppb/ppm). This low value clearly indicates the dominance of CO<sub>2</sub> over the study region. The reported  $\Delta\text{CH}_4/\Delta\text{CO}_2$  values from some of the rural sites viz Canadian Arctic and Hateruma Island (China) is of the order 12.2 and 10 ppb/ppm respectively (Worthy et al., 2009; Tohjima et al., 2014). Average  $\Delta\text{CH}_4/\Delta\text{CO}_2$  ratio during winter, pre-monsoon, monsoon and post-monsoon are 9.40, 6.40, 4.40, and 8.20 ppb respectively. Monthly average, of  $\Delta\text{CH}_4/\Delta\text{CO}_2$ , is relatively high from late post-monsoon to winter, when the biotic activity is relatively dormant (Tohjima et al., 2014). During pre-monsoon decrease in  $\Delta\text{CH}_4/\Delta\text{CO}_2$  ratio indicates the enhancement of CO<sub>2</sub> relative to that of CH<sub>4</sub>.

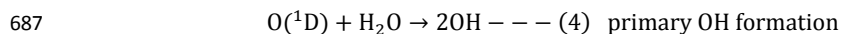
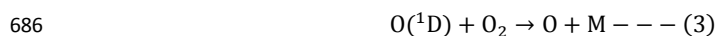
#### **4.5.4.6 Methane (CH<sub>4</sub>) sink mechanism**

Methane (CH<sub>4</sub>) is the most powerful greenhouse gas after CO<sub>2</sub> in the atmosphere due to its strong positive radiative forcing (IPCC, AR5). Atmospheric CH<sub>4</sub> is mainly (70-80%) from biological origin produced in anoxic environments, by anaerobic digestion of organic matter (Crutzen and Zimmermann, 1991). The major CH<sub>4</sub> sink is oxidation by hydroxyl radicals (OH), which accounts for 90 % of CH<sub>4</sub> sink (Vaghjiani and Ravishankara, 1991; Kim et al., 2015). OH radicals are very reactive and are responsible for the oxidation of almost all gases in the

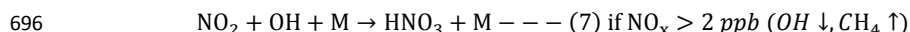
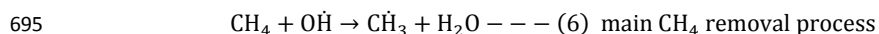
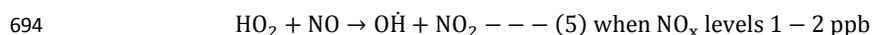
atmosphere. Primary source for OH radical formation in the atmosphere is photolysis of ozone (O<sub>3</sub>) and water vapor (H<sub>2</sub>O). Eisele et al., (1997) defined primary and secondary source of OH radicals in the atmosphere. Primary source of OH radical is as follows;



where O(<sup>1</sup>D) is electronically excited atom



Removal of CH<sub>4</sub> is constrained by the presence of OH radicals in the atmosphere. A 1 min time series analysis of CH<sub>4</sub>, NO<sub>x</sub>, O<sub>3</sub> and H<sub>2</sub>O and associated wind vector for August 2014 to understand the CH<sub>4</sub> chemistry is shown in Figure 710a and Figure 710b. Low NO<sub>x</sub> (1-2 ppb) values are shown in horizontal elliptical region of Figure 710a and observed corresponding low CH<sub>4</sub> (1.80 ppm) concentrations. The low NO<sub>x</sub> in turn produces high OH radicals in the atmosphere due to conversion of HO<sub>2</sub> radical by NO, which removes CH<sub>4</sub> through oxidation process as shown below.



Crutzen and Zimmermann, (1991) and Eisele et al., (1997) observed that at low NO<sub>x</sub> (0.5-2.0 ppb) levels most HO<sub>x</sub> family radicals such as HO<sub>2</sub> and peroxy radicals (RO<sub>2</sub>) react with NO to form OH radicals. Therefore OH radicals are much higher in the case of low NO<sub>x</sub>. When NO<sub>x</sub> levels increase more than 2 ppb, most of the OH radicals react with NO<sub>2</sub> to form nitric acid (HNO<sub>3</sub>). In first order, the levels of CH<sub>4</sub> in the atmosphere depend on the levels of NO<sub>x</sub> though the production of OH radicals in the atmosphere is still uncertain. Figure 710a and 710b showed high CH<sub>4</sub>, H<sub>2</sub>O, O<sub>3</sub> and NO<sub>x</sub> during a few days in August 2014. High concentrations of CH<sub>4</sub>, NO<sub>x</sub> and other gases are observed in the eastern direction of study site. Very high NO<sub>x</sub> levels above 10 ppb are observed and subsequently CH<sub>4</sub> concentrations also increased to 2.40 ppm from 1.80 ppm. In the eastern

direction of study site a national highway and single line broad gauge railway network are present which act as possible sources of NO<sub>x</sub>, CH<sub>4</sub> and CO<sub>2</sub>. Increase in emissions of NO<sub>x</sub> causes decline in the levels of OH radicals and subsequently observed high CH<sub>4</sub> over the study region.

#### 4.6 Influence of vegetation on GHG's.

In India cropping season is classified into (i) Kharif and (ii) Rabi based on the onset of monsoon. The kharif season is from July to October during the south west monsoon and Rabi season is from October to March (Avadhesh Koshal, 2013). NDVI being one of the indicators of vegetation change, monthly variations of CO<sub>2</sub> and CH<sub>4</sub> against NDVI is studied to understand the impact of land use land cover on mixing ratios of CO<sub>2</sub> and CH<sub>4</sub>. Monthly changes in NDVI, CO<sub>2</sub> and CH<sub>4</sub> are shown in Figure 8. Monthly mean of GHG's represented in this analysis is calculated from daily day time (10-16 LT) mean. Maximum NDVI of 0.60 corresponding to the minimum CO<sub>2</sub> concentration (about 382 ppm) is observed in September. NDVI showed inverse relationship with CO<sub>2</sub>, mainly due to change in vegetation which affects the CO<sub>2</sub> concentrations. Initially during the month of June vegetation start increasing with availability of water and as vegetation increases, concentration. Similarly, The main source for CH<sub>4</sub> emissions are soil microbial (Stefanie Kirschke et al., 2013) activity which are more active during monsoon and post monsoon seasons. High (low) soil moisture and NDVI is observed in monsoon (pre monsoon) seasons (Figure 9a and b). The predominating factors which controls the soil emissions of CO<sub>2</sub>, CH<sub>4</sub> are moisture content, soil temperature, vegetation and soil respiration (Smith et al., 2003; Jones et al., 2005; Chen et al., 2010) respectively.

Biomass burning (forest fire and crop residue burning) is one of the major sources of gaseous pollutants such as carbon monoxide (CO), methane (CH<sub>4</sub>), nitrous oxides (NO<sub>x</sub>) and hydrocarbons in the troposphere (Crutzen et al., 1990, 1985; Sharma et al., 2010). In order to study the role of biomass burning on GHG's a case study is discussed. Figure 10a shows the spatial distribution of MODIS derived fire counts over Indian region during 14-21 April 2014 with air mass trajectories ending over study area over layed on it at different altitudes viz. 1000m, 2000m and 4000m respectively. Analysis of the figure shows a number of potential fire locations on the north western and south eastern side of study location and trajectories indicates its possible transport to study area. Daily mean variation of GHGs during the month of April 2014 (Figure

Formatted: Strikethrough



10b) indicates an enhancement in GHGs during the same period (14–21 April 2014). Analysis reveals that CO<sub>2</sub> and CH<sub>4</sub> has increased by ~2% and ~0.06% respectively during event days with respect to monthly mean. This analysis reveals that long range / regional transported biomass burning have a role in enhancement of GHGs over study site. Further to understand the seasonal variation of biomass burning contribution to GHGs we analysed over study site we have analysed GHG's emissions from biomass burning using long term (2003–2013) Fire Energetics and Emissions Research version 1.0 (FEER-v1) data over study area. Emission coefficient (C<sub>e</sub>) products during biomass burning is developed from coincident measurements of fire radiative power (FRP) and AOD from MODIS Aqua and Terra satellites (Ichoku and Ellison, 2014). Figure 10c shows seasonal variation of CO<sub>2</sub> emission due to biomass burning over the study site. Enhancement in CO<sub>2</sub> emission is seen during pre-monsoon months; which also supports earlier observation (Figure 2a). This analysis reveals that biomass burning has a role in pre-monsoon enhancement of CO<sub>2</sub> over study site. For a qualitative analysis of this long-range transport, we have analysed air mass trajectories ending over study site during different seasons.

Formatted: Subscript

#### 4.7 Long range circulations

To understand the role of long range circulation, we separated the trajectory into 4 clusters based on their pathway, namely North-East (N-E), North-West (N-W), South-East (S-E), South-West (S-W). The main criterion of trajectory clustering is to minimize the variability among trajectories and maximize variability among clusters. Cluster mean trajectories of air mass and their percentage contribution to the total calculated for each season over the study period at 3 Km altitude are depicted in Figure 911. Majority of air mass trajectories during winter (~44%), pre-monsoon (~64%), monsoon (~80%) and post-monsoon (~41%) are originating from NW parts of the study site. For a comprehensive analysis, percentage occurrences of cluster mean trajectories of air mass over study area during different season at different altitudes are also tabulated in Table 4. During post-monsoon to early pre-monsoon periods which are generally the post-harvest period for some of the crops agriculture residue burning which are quite common in the NW and NE regions part of India (Sharma et al, 2010). Our analysis reveals that during this period majority of air mass reaching the study site at different altitudes come from this part of the country.

## 5. Conclusions

The present study analysed the seasonal variations of atmospheric GHG<sup>2</sup>s (CO<sub>2</sub> and CH<sub>4</sub>) and associated prevailing meteorology over Shadnagar, a suburban site of Central India during the period 2014. The salient findings of the study are the following:

- Irrespective of seasons, major sources for CO<sub>2</sub> are soil respiration and anthropogenic emissions while vegetation acts as a main sink. Whereas the major source and sink for CH<sub>4</sub> are vegetation and presence of hydroxyl (OH) radicals. In addition, boundary layer dynamics and long range transport also plays a vital role on GHGs mixing ratios.
- The annual mean of CO<sub>2</sub> and CH<sub>4</sub> over the study region ~~are~~<sup>is</sup> found to be 394±2.92 ppm and 1.92±0.07 ppm ( $\mu\pm 1\sigma$ ) respectively. CO<sub>2</sub> and CH<sub>4</sub> showed a significant seasonal variation during the study period. Maximum (Minimum) CO<sub>2</sub> is observed during Pre-monsoon (Monsoon), while CH<sub>4</sub> recorded maximum during post-monsoon and minimum in monsoon. Seasonal analysis of FEER data also showed maximum emission of CO<sub>2</sub> due to biomass burning during pre-monsoon months which indicates the influence of biomass burning on local emissions.
- CO<sub>2</sub> and CH<sub>4</sub> showed consistent diurnal behavior in spite of their significant seasonal variations, with an observed morning (06:00 IST) maxima, followed by afternoon minima (14:00 IST) and enhancing in the late evening (~22:00 IST).
- Correlation coefficient ( $R_s$ ) between wind speed and CO<sub>2</sub> during pre-monsoon, monsoon, post-monsoon and winter is 0.56, 0.32, 0.06 and 0.67 respectively. While for CH<sub>4</sub> it is found be 0.28, 0.71, 0.21, and 0.60 respectively. Negative correlation indicates that the influence of local sources on GHG<sup>2</sup>s, however, poor correlation coefficients during different seasons suggest the role of regional/local transport.
- CO<sub>2</sub> showed a positive correlation with temperature during all seasons except during winter. ~~Where as~~<sup>Whereas</sup> CH<sub>4</sub> showed a weak positive correlation with temperature during pre-monsoon and post-monsoon, while showing a weak negative correlation during monsoon and winter.
- CO<sub>2</sub> and CH<sub>4</sub> showed a strong positive correlation during winter, pre-monsoon, monsoon and post-monsoon with  $R_s$  equal to 0.80, 0.80, 0.61 and 0.72 respectively. This clearly

Formatted: Font: (Default) Times New Roman, 12 pt

indicates [common anthropogenic sources for these gases](#),~~the seasonal variations in~~  
~~source-sink mechanisms of CO<sub>2</sub> and CH<sub>4</sub> respectively.~~  
◆ ~~Presence of OH radicals has been implicitly confirmed as a major sink of CH<sub>4</sub> over the~~  
~~study region.~~

## Acknowledgment

This work was part of the Atmospheric CO<sub>2</sub> Retrieval and Monitoring (ACRM) under National Carbon Project (NCP) of ISRO-GBP. [Authors sincerely acknowledge Mr. Biswadip Gharai, ACSG/ECSA for providing LULC data and to Mr. Mallikarjun, ACSG/ECSA for his support in data collection.](#) We thank D & PQE division of NRSC and Mrs. Sujatha P, ACSG for sharing AWS and boundary layer data. The authors are grateful to the AT-CTM project of ISRO-GBP for providing the O<sub>3</sub> and NO<sub>x</sub> analyzers. We would also like to thank [HYSPLIT](#), [ECMWF-ERA](#), MODIS and COSMIC team for providing scientific data sets used in this study. [We also thankful to anonymous referees and the editor for providing constructive suggestions which certainly improved the quality of manuscript.](#)

## References

- Ao, C. O., Waliser, D. E., Chan, S. K., Li, J. L., Tian, B., Xie, F., & Mannucci, A. J. Planetary boundary layer heights from GPS radio occultation refractivity and humidity profiles. *Journal of Geophysical Research: Atmospheres* (1984–2012), 117(D16), (2012).
- [Aurela M, Lohila A, Tuovinen JP, Hatakka J, Riutta T, Laurila T \(2009\) Carbon dioxide exchange on a northern boreal fen. \*Boreal Environment Research\* 14\(4\): 699-710](#)
- Baer, D. S., Paul, J. B., Gupta, M., & O'Keefe, A. Sensitive absorption measurements in the near-infrared region using off-axis integrated cavity output spectroscopy. In *International Symposium on Optical Science and Technology* (pp. 167-176). International Society for Optics and Photonics, (2002).
- Berman, E. S., Fladeland, M., Liem, J., Kolyer, R., & Gupta, M. Greenhouse gas analyzer for measurements of carbon dioxide, methane, and water vapor aboard an unmanned aerial vehicle. *Sensors and Actuators B: Chemical*, 169, 128-135, (2012).

822 Chen, H., Wu, N., Wang, Y., & Peng, C. Methane is an Important Greenhouse Gas. Methane  
823 Emissions from Unique Wetlands in China: Case Studies, Meta Analyses and Modelling, chapter  
824 1, (2015).

825 Crutzen, P. J., & Andreae, M. O. Biomass burning in the tropics: Impact on atmospheric chemistry  
826 and biogeochemical cycles. *Science*, 250(4988), 1669-1678, (1990).

827 Crutzen, P. J., A. C. Delany, J. Greenberg, P. Haagenson, L. Heidt, R. Lueb, W. Pollock, Wartburg  
828 Seiler, A. Wartburg, and P. Zimmerman. "Tropospheric chemical composition measurements in  
829 Brazil during the dry season." *Journal of Atmospheric Chemistry* 2, no. 3 (1985): 233-256.

830 Draxler RR, Rolph GD. HySPLIT (Hybrid Single Particle Lagrangian Integrated Trajectory)  
831 Model access via NOAA ARL READY website (<http://www.arl.noaa.gov/ready/hysplit4.html>),  
832 NOAA Air Resources Laboratory. *Silver Spring, MD*. 2003.

833  
834 Eisele, F. L., Mount, G. H., Tanner, D., Jefferson, A., Shetter, R., Harder, J. W., & Williams, E. J.  
835 Understanding the production and interconversion of the hydroxyl radical during the Tropospheric  
836 OH Photochemistry Experiment. *Journal of Geophysical Research: Atmospheres* (1984–2012),  
837 102(D5), 6457-6465, (1997).

838 Fang, S. X., L. X. Zhou, P. P. Tans, P. Ciais, M. Steinbacher, L. Xu, and T. Luan. "In situ  
839 measurement of atmospheric CO<sub>2</sub> at the four WMO/GAW stations in China." *Atmospheric  
840 Chemistry and Physics* 14, no. 5 (2014): 2541-2554.

841 Fang, S. X., P. P. Tans, M. Steinbacher, L. X. Zhou, and T. Luan. "Study of the regional CO<sub>2</sub> mole  
842 fractions filtering approach at a WMO/GAW regional station in China." *Atmospheric  
843 Measurement Techniques Discussions* 8, no. 7 (2015).

844 [Fearnside, Philip M. "Global warming and tropical land use change: greenhouse gas emissions  
845 from biomass burning, decomposition and soils in forest conversion, shifting cultivation and  
846 secondary vegetation." \*Climatic change\* 46, no. 1-2 \(2000\): 115-158.](#)

847 Frankenberg, Christian, Peter Bergamaschi, André Butz, Sander Houweling, Jan Fokke Meirink,  
848 Justus Notholt, Anna Katinka Petersen, Hans Schrijver, Thorsten Warneke, and Ilse Aben.  
849 "Tropical methane emissions: A revised view from SCIAMACHY onboard ENVISAT."  
850 *Geophysical Research Letters* 35, no. 15 (2008).

851 Garg, A., Bhattacharya, S., Shukla, P. R., & Dadhwal, V. K. Regional and sectoral assessment of  
852 greenhouse gas emissions in India. *Atmospheric Environment*, 35(15), 2679-2695, (2001).

853  
854 Gaur, A., Tripathi, S. N., Kanawade, V. P., Tare, V., & Shukla, S. P. Four-year measurements of  
855 trace gases (SO<sub>2</sub>, NO<sub>x</sub>, CO, and O<sub>3</sub>) at an urban location, Kanpur, in Northern India. *Journal of  
856 Atmospheric Chemistry*, 71(4), 283-301, (2014).

857

858 Gilmanov, T. G., Johnson, D. A., Saliendra, N. Z., Akshalov, K., & Wylie, B. K. Gross primary  
 859 productivity of the true steppe in Central Asia in relation to NDVI: scaling up CO<sub>2</sub> fluxes.  
 860 Environmental Management, 33(1), S492-S508, (2004).

861 Goroshi, S. K., Singh, R. P., Panigrahy, S., & Parihar, J. S. Analysis of seasonal variability of  
 862 vegetation and methane concentration over India using SPOT-VEGETATION and ENVISAT-  
 863 SCIAMACHY data. Journal of the Indian Society of Remote Sensing, 39(3), 315-321, (2011).

864 Hassan, A. G. A. Diurnal and Monthly Variations in Atmospheric CO<sub>2</sub> Level in Qena, Upper  
 865 Egypt. Resources and Environment, 5(2), 59-65, (2015).

866 [Hayashida, S., Ono, A., Yoshizaki, S., Frankenberg, C., Takeuchi, W., & Yan, X. \(2013\). Methane](#)  
 867 [concentrations over Monsoon Asia as observed by SCIAMACHY: Signals of methane emission](#)  
 868 [from rice cultivation. Remote Sensing of Environment, 139, 246-256.](#)

869 [Huang, J.\\*, W. Zhang, J. Zuo, J. Bi, J. Shi, X. Wang, Z. Chang, Z. Huang, S. Yang, B. Zhang, G.](#)  
 870 [Wang, G. Feng, J. Yuan, L. Zhang, H. Zuo, S. Wang, C. Fu and J. Chou, 2008: An overview of](#)  
 871 [the Semi-Arid Climate and Environment Research Observatory over the Loess Plateau. Advances](#)  
 872 [in Atmospheric Sciences, 25\(6\), 1-16.](#)

873 [Huang, J., Yu, H., Guan, X., Wang, G., & Guo, R. \(2015\). Accelerated dryland expansion under](#)  
 874 [climate change. Nature Climate Change, doi:10.1038/nclimate2837.](#)

875 Ichoku, C., & Ellison, L. Global top-down smoke-aerosol emissions estimation using satellite fire  
 876 radiative power measurements. Atmospheric Chemistry and Physics, 14(13), 6643-6667, (2014).

877 Intergovernmental Panel on Climate Change (IPCC). Climate Change: The IPCC Scientific  
 878 Assessment, edited by J. T. Houghton, G. J. Jerkins and J. J. Ephraums. Cambridge University  
 879 Press. New York, (IPCC, 1990).

880 James, M. E., & Kalluri, S. N. The Pathfinder AVHRR land data set: an improved coarse resolution  
 881 data set for terrestrial monitoring. International Journal of Remote Sensing, 15(17), 3347-3363,  
 882 (1994).

883 [Jing, X., Huang, J., Wang, G., Higuchi, K., Bi, J., Sun, Y., ... & Wang, T. \(2010\). The effects of](#)  
 884 [clouds and aerosols on net ecosystem CO<sub>2</sub> exchange over semi-arid Loess Plateau of Northwest](#)  
 885 [China. Atmospheric Chemistry and Physics, 10\(17\), 8205-8218.](#)

886 Jones, C., McConnell, C., Coleman, K., Cox, P., Falloon, P., Jenkinson, D., & Powlson, D. Global  
 887 climate change and soil carbon stocks; predictions from two contrasting models for the turnover  
 888 of organic carbon in soil. Global Change Biology, 11(1), 154-166, (2005).

894 Keppler, F., Hamilton, J. T., Braß, M., & Röckmann, T. Methane emissions from terrestrial plants  
895 under aerobic conditions. *Nature*, 439(7073), 187-191, (2006).

896 Kim, H. S., Chung, Y. S., Tans, P. P., & Dlugokencky, E. J. Decadal trends of atmospheric methane  
897 in East Asia from 1991 to 2013. *Air Quality, Atmosphere & Health*, 8(3), 293-298, (2015).

898 King, M. D., Kaufman, Y. J., Menzel, W. P., & Tanre, D. Remote sensing of cloud, aerosol, and  
899 water vapor properties from the Moderate Resolution Imaging Spectrometer (MODIS).  
900 *Geoscience and Remote Sensing, IEEE Transactions on*, 30(1), 2-27, (1992).

901 Kirschke, Stefanie., Bousquet, Philippe., Ciais, Philippe., Saunois, Marielle., Canadell, Josep G.,  
902 Dlugokencky, Edward J., Bergamaschi, Peter., Bergmann, Daniel., Blake, Donald R., Bruhwiler,  
903 Lori., Cameron-Smith, Philip., Castaldi, Simona., Chevallier, Frédéric., Feng, Liang., Fraser,  
904 Annemarie., Heimann, Martin., Hodson, Elke L., Houweling, Sander., Josse, Béatrice., Fraser,  
905 Paul J., Krummel, Paul B., Lamarque, Jean-François., Langenfelds, Ray L., Quéré, Corinne Le.,  
906 Naik, Vaishali., O'Doherty, Simon., Palmer, Paul I., Pison, Isabelle., Plummer, David., Poulter,  
907 Benjamin., Prinn, Ronald G., Rigby, Matt., Ringeval, Bruno., Santini, Monia., Schmidt,  
908 Martina., Shindell, Drew T., Simpson, Isobel J., Spahni, Renato., Steele, L. Paul., Strode, Sarah  
909 A., Sudo, Kengo., Szopa, Sophie., Werf, Guido R. van der., Voulgarakis, Apostolos., Weele,  
910 Michiel van., Weiss, Ray F., Williams, Jason E., Guang, Zeng. Three decades of global methane  
911 sources and sinks, *Nature Geoscience*, volume 6, (2013), doi: 10.1038/NGEO1955.

912 Koshal. A. K. Spatial temporal climatic change variability of cropping system in western Uttar  
913 Pradesh, *International Journal of Remote Sensing & Geoscience*, volume 2, issue 3, (2013).

914 Lewis, A. C., Evans, M. J., Hopkins, J. R., Punjabi, S., Read, K.A., Purvis, R. M., Andrews, S. J.,  
915 Moller, S. J., Carpenter, L.J., Lee, J. D., Rickard, A. R., Palmer, P. I., and Parrington, M.: The  
916 influence of biomass burning on the global distribution of selected non-methane organic  
917 compounds, *Atmos. Chem. Phys.*, 13, 851–867, doi:10.5194/acp-13-851-2013, 2013.

918 Liu, Yang, Xiufeng Wang, Meng Guo, Hiroshi Tani, Nobuhiro Matsuoka, and Shinji Matsumura.  
919 "Spatial and temporal relationships among NDVI, climate factors, and land cover changes in  
920 Northeast Asia from 1982 to 2009." *GIScience & Remote Sensing* 48, no. 3 (2011): 371-393.

921 Machida, T., K. Kita, Y. Kondo, D. Blake, S. Kawakami, G. Inoue, and T. Ogawa. "Vertical and  
922 meridional distributions of the atmospheric CO<sub>2</sub> mixing ratio between northern midlatitudes and  
923 southern subtropics." *Journal of Geophysical Research: Atmospheres* (1984–2012) 107, no. D3  
924 (2002): BIB-5.

925 Mahesh, P., N. Sharma, V. K. Dadhwal, P. V. N. Rao, and B. V. Apparao. "Impact of Land-Sea  
 926 Breeze and Rainfall on CO<sub>2</sub> Variations at a Coastal Station. J Earth Sci Clim Change 5: 201. doi:  
 927 10.4172/2157-7617.1000201 Volume 5. Issue 6. (2014).

928 Mahesh. P, Sreenivas. G, Rao.P.V.N., Dadhwal.V.K.,Sai Krishna. S.V.S. and Mallikarjun. K:  
 929 High precision surface level CO<sub>2</sub> and CH<sub>4</sub> using Off-Axis Integrated Cavity Output Spectroscopy  
 930 (OA-ICOS) over Shadnagar, India, International Journal of Remote Sensing, (2015),  
 931 doi:10.1080/01431161.2015.1104744.

932 Miller, John B., Luciana V. Gatti, Monica TS d'Amelio, Andrew M. Crotnell, Edward J.  
 933 Dlugokencky, Peter Bakwin, Paulo Artaxo, and Pieter P. Tans. "Airborne measurements indicate  
 934 large methane emissions from the eastern Amazon basin." Geophysical Research Letters 34, no.  
 935 10 (2007).

936 Monastersky, Richard. "Global carbon dioxide levels near worrisome milestone." Nature 497, no.  
 937 7447 (2013): 13-14.

938 [Nair, V. S., Moorthy, K. K., Alappattu, D. P., Kunhikrishnan, P. K., George, S., Nair, P. R., &](#)  
 939 [Niranjan, K. \(2007\). Wintertime aerosol characteristics over the Indo-Gangetic Plain \(IGP\):](#)  
 940 [Impacts of local boundary layer processes and long-range transport. Journal of Geophysical](#)  
 941 [Research: Atmospheres \(1984–2012\), 112\(D13\).](#)

942 Newman, S., Jeong, S., Fischer, M. L., Xu, X., Haman, C. L., Lefer, B., Alvarez, S., Rappenglueck,  
 943 B., Kort, E. A., Andrews, A. E., Peischl, J., Gurney, K. R., Miller, C. E., and Yung, Y. L.: Diurnal  
 944 tracking of anthropogenic CO<sub>2</sub> emissions in the Los Angeles basin megacity during spring, Atmos.  
 945 Chem. Phys., 13, 4359–4372, 2013, doi:10.5194/acp-13-4359-2013.

946 Nishanth, T., K. M. Praseed, M. K. Satheesh Kumar, and K. T. Valsaraj. "Observational study of  
 947 surface O<sub>3</sub>, NO<sub>x</sub>, CH<sub>4</sub> and total NMHCs at Kannur, India." Aerosol. Air. Qual. Res 14 (2014):  
 948 1074-1088.

949 Pan, X. L., Kanaya, Y., Wang, Z. F., Liu, Y., Pochanart, P., Akimoto, H., Sun, Y. L., Dong, H. B.,  
 950 Li, J., Irie, H., and Takigawa, M.: Correlation of black carbon aerosol and carbon monoxide in the  
 951 high-altitude environment of Mt. Huang in Eastern China, Atmos. Chem. Phys., 11, 9735-9747,  
 952 doi:10.5194/acp-11-9735-2011, 2011

953 Paul, J. B., Lapson, L., & Anderson, J. G.. Ultrasensitive absorption spectroscopy with a high-  
 954 finesse optical cavity and off-axis alignment. Applied Optics, 40(27), 4904-4910, (2001).

955 Patil, M. N., T. Dharmaraj, R. T. Waghmare, T. V. Prabha, and J. R. Kulkarni. "Measurements of  
 956 carbon dioxide and heat fluxes during monsoon-2011 season over rural site of India by eddy  
 957 covariance technique." Journal of Earth System Science 123, no. 1 (2014): 177-185.

958 Pielke, Roger A., Gregg Marland, Richard A. Betts, Thomas N. Chase, Joseph L. Eastman, John  
959 O. Niles, and Steven W. Running. "The influence of land-use change and landscape dynamics on  
960 the climate system: relevance to climate-change policy beyond the radiative effect of greenhouse  
961 gases." *Philosophical Transactions of the Royal Society of London A: Mathematical, Physical and  
962 Engineering Sciences* 360, no. 1797 (2002): 1705-1719.

963 Ramachandran, S., and T. A. Rajesh. "Black carbon aerosol mass concentrations over Ahmedabad,  
964 an urban location in western India: comparison with urban sites in Asia, Europe, Canada, and the  
965 United States." *Journal of Geophysical Research: Atmospheres* (1984–2012) 112, no. D6 (2007).  
966 Salomonson, Vincent V., W. L. Barnes, Peter W. Maymon, Harry E. Montgomery, and Harvey  
967 Ostrow. "MODIS: Advanced facility instrument for studies of the Earth as a system." *Geoscience  
968 and Remote Sensing, IEEE Transactions on* 27, no. 2 (1989): 145-153.

969 Smith, K. A., Ball, T., Conen, F., Dobbie, K. E., Massheder, J., & Rey, A. Exchange of greenhouse  
970 gases between soil and atmosphere: interactions of soil physical factors and biological processes.  
971 *European Journal of Soil Science*, 54(4), 779-791, (2003).

972 Schneising, O., M. Buchwitz, J. P. Burrows, H. Bovensmann, P. Bergamaschi, and W. Peters.  
973 "Three years of greenhouse gas column-averaged dry air mole fractions retrieved from satellite—  
974 Part 2: Methane." *Atmos. Chem. Phys* 9, no. 2 (2009): 443-465.

975 Sharma Neerja, Dadhwal, V.K., Kant, Y., Mahesh, P., Mallikarjun, K., Gadavi, Harish, Sharma,  
976 Anand., Ali, M.M. Atmospheric CO<sub>2</sub> Variations in Two Contrasting Environmental Sites Over  
977 India. *Air, Soil and Water Research* 2014:7 61–68, (2014), doi:10.4137/ASWR.S13987.

978 Sharma, Anu Rani, Shailesh Kumar Kharol, K. V. S. Badarinath, and Darshan Singh. "Impact of  
979 agriculture crop residue burning on atmospheric aerosol loading—a study over Punjab State,  
980 India." In *Annales geophysicae: atmospheres, hydrospheres and space sciences*, vol. 28, no. 2, p.  
981 367. 2010.

982 Sharma, Neerja, Rabindra K. Nayak, Vinay K. Dadhwal, Yogesh Kant, and Meer M. Ali.  
983 "Temporal variations of atmospheric CO<sub>2</sub> in Dehradun, India during 2009." *Air, Soil and Water  
984 Research* 6 (2013): 37.

985 Stocker, T.F., Qin, D., Plattner, G.K., Alexander, L.V., Allen, S.K., Bindoff, N.L., Bréon, F.M.,  
986 Church, J.A., Cubasch, U., Emori, S., Forster, P., Friedlingstein, P., Gillett, N., Gregory, J.M.,  
987 Hartmann, D.L., Jansen, E., Kirtman, B., Knutti, R., Krishna Kumar, K., Lemke, P., Marotzke, J.,  
988 Masson-Delmotte, V., Meehl, G.A., Mokhov, I.I., Piao, S., Ramaswamy, V., Randall, D., Rhein,  
989 M., Rojas, M., Sabine, C., Shindell, D., Talley, L.D., Vaughan D.G., and Xie, S.P. Technical  
990 Summary. In: *Climate Change 2013: The Physical Science Basis. Contribution of Working Group  
991 I to the Fifth Assessment Report of the Intergovernmental Panel on Climate Change* [Stocker, T.F.,  
992 D. Qin, G.-K. Plattner, M. Tignor, S.K. Allen, J. Boschung, A. Nauels, Y. Xia, V. Bex and P.M.  
993 Midgley (eds.)]. Cambridge University Press, Cambridge, United Kingdom and New York, NY,  
994 USA, (2013).



995 [Shea, S.J.O, G. Allen<sup>1</sup>, M. W. Gallagher, S. J.-B. Bauguitte, S. M. Illingworth, M. Le Breton, J.](#)  
996 [B. A. Muller,C. J. Percival, A. T. Archibald, D. E. Oram, M. Parrington,<sup>\\*</sup>, P. I. Palmer. and A. C.](#)  
997 [Lewis. Airborne observations of trace gases over boreal Canada during BORTAS: campaign](#)  
998 [climatology, air mass analysis and enhancement ratios. Atmos. Chem. Phys., 13, 12451–12467,](#)  
999 [2013 atmos-chem-phys.net/13/12451/2013/ doi:10.5194/acp-13-12451-2013](#)

1000 Stohl, Andreas, Markus Hittenberger, and Gerhard Wotawa. "Validation of the Lagrangian particle  
1001 dispersion model FLEXPART against large-scale tracer experiment data." *Atmospheric*  
1002 *Environment* 32, no. 24 (1998): 4245-4264.

1003 [Stull, R. B. \(1988\). Similarity theory. In \*An Introduction to Boundary Layer Meteorology\* \(pp.](#)  
1004 [347-404\). Springer Netherlands.](#)

1005

1006

1007 Taylor J. *An Introduction to Error Analysis: The Study of Uncertainties in Physical Measurement*,  
1008 University Science Books, And ISBN: 093570275X (ISBN13: 9780935702750), (1997).

1009 Thum, T., T. Aalto, T. Laurila, M. Aurela, J. Hatakka, Anders Lindroth, and T. Vesala. "Spring  
1010 initiation and autumn cessation of boreal coniferous forest CO<sub>2</sub> exchange assessed by  
1011 meteorological and biological variables." *Tellus B* 61, no. 5 (2009): 701-717.

1012 Tohjima, Y., Kubo, M., Minejima, C., Mukai, H., Tanimoto, H., Ganshin, A., Maksyutov, S.,  
1013 Katsumata, K., Machida, T., and Kita, K.: Temporal changes in the emissions of CH<sub>4</sub> and CO  
1014 from China estimated from CH<sub>4</sub> / CO<sub>2</sub> and CO / CO<sub>2</sub> correlations observed at Hateruma Island,  
1015 *Atmos. Chem. Phys.*, 14, 1663-1677, doi:10.5194/acp-14-1663-2014, 2014.

1016

1017 Vaghjiani, Ghanshyam L., and A. R. Ravishankara. "New measurement of the rate coefficient for  
1018 the reaction of OH with methane." *Nature* 350, no. 6317 (1991): 406-409.

1019 Wang, B-R., X-Y. Liu, and J-K. Wang. "Assessment of COSMIC radio occultation retrieval  
1020 product using global radiosonde data." *Atmospheric Measurement Techniques* 6, no. 4 (2013):  
1021 1073-1083.

1022 [Wang, G., J. Huang\\*, W. Guo, J. Zuo, J. Wang, J. Bi, Z. Huang, and J. Shi, 2010: Observation](#)  
1023 [analysis of land-atmosphere interactions over the Loess Plateau of northwest China, J. Geophys.](#)  
1024 [Res., 115, D00K17,doi:10.1029/2009JD013372.](#)

1025 Worthy, Douglas EJ, Elton Chan, Misa Ishizawa, Douglas Chan, Christian Poss, Edward J.  
1026 Dlugokencky, Shamil Maksyutov, and Ingeborg Levin. "Decreasing anthropogenic methane  
1027 emissions in Europe and Siberia inferred from continuous carbon dioxide and methane  
1028 observations at Alert, Canada." *Journal of Geophysical Research: Atmospheres* (1984–2012) 114,  
1029 no. D10 (2009).

1030  
1031

1032 Yunck, Thomas P., Liu Chao-Han, and Randolph Ware. "A history of GPS sounding." Terrestrial  
1033 Atmospheric and Oceanic Sciences 11, no. 1 (2000): 1-20.

1034

1035

1036

1037

1038

1039

1040

1041

1042

1043

1044 **Table 1** Data used

1045

1046

1047

1048

1049

1050

1051

1052

1053

1054

1055

1056

1057  
1058  
1059

Sensor	Period	Parameter	resolution	Source
GGA-24EP	Jan-2014 to Dec 2014	CO <sub>2</sub> ,CH <sub>4</sub> and H <sub>2</sub> O	1 Hz time	ASL,NRSC
42i-NO-NO <sub>2</sub> -NO <sub>x</sub>	Jul-2014 to Sep-2014	NO <sub>x</sub> (=NO+N O <sub>2</sub> )	1 min time	ASL,NRSC
49i-O <sub>3</sub>	Jul-2014 to Sep-2014	O <sub>3</sub>	1 min time	ASL,NRSC
AWS	Jan-2014 to Dec-2014	WS,WD,AT,RH	60 min time	NRSC
Terra/MODIS	Jan-2014 to Dec-2014	NDVI	5 Km horizontal	<a href="http://ladsweb.nascom.nasa.gov/data/search.html">http://ladsweb.nascom.nasa.gov/data/search.html</a>
COSMIC-IDVAR	Jul-2013 to Jun-2014	Refractivity (N)	0.1 Km vertical	
HYSPLIT	Jan-2014 to Dec-2014	Backward trajectory	5 day isentropic model (1km to 4 km)	<a href="http://ww.arl.noaa.gov/ready/hysplit4.html">http://ww.arl.noaa.gov/ready/hysplit4.html</a>
FEER v1	Jan-2013 to Dec-2013	fire radiative power (FRP)		<a href="http://ladsweb.nascom.nasa.gov/data/search.html">http://ladsweb.nascom.nasa.gov/data/search.html</a>

1060  
1061  
1062  
1063  
1064  
1065  
1066  
1067  
1068  
1069  
1070  
1071

**Table 2** Statistical correlation between CO<sub>2</sub> and CH<sub>4</sub>

<u>S.No</u>	<u>Seasons</u>	<u>Correlation coefficient (R)</u>	<u>Slope</u> $\left(\frac{Y_{CH_4} (ppm)}{X_{CO_2} (ppm)}\right)$	<u><math>\Psi_{slope}</math></u> (ppm)	<u><math>\Psi_{v-int}</math></u> (ppm)
<u>1</u>	<u>Monsoon (JJAS)</u>	<u>0.61</u>	<u>0.005</u>	<u>0.00015</u>	<u>1.91</u>
<u>2</u>	<u>Post- monsoon (OND)</u>	<u>0.72</u>	<u>0.0065</u>	<u>0.00014</u>	<u>1.52</u>
<u>3</u>	<u>Winter (JF)</u>	<u>0.80</u>	<u>0.0085</u>	<u>0.00018</u>	<u>9.13</u>
<u>4</u>	<u>Pre- monsoon (MAM)</u>	<u>0.80</u>	<u>0.0059</u>	<u>0.00021</u>	<u>2.73</u>

**Table 23** Seasonal amplitudes of CO<sub>2</sub> and CH<sub>4</sub> over study region arriving from different directions

Wind Direction	Winter $\frac{CO_2}{CH_4}$ (ppm)	Pre-monsoon $\frac{CO_2}{CH_4}$ (ppm)	Monsoon $\frac{CO_2}{CH_4}$ (ppm)	Post-monsoon $\frac{CO_2}{CH_4}$ (ppm)
0-45	399.85/1.98	410.37/1.94	400.72/1.91	395.13/2.02
45-90	391.66/1.94	399.59/1.89	388.82/1.91	390.23/1.98
90-135	391.57/1.93	397.79/1.87	388.99/1.87	389.06/1.97
135-180	389.34/1.89	393.87/1.85	391.81/1.86	387.69/1.97
180-225	391.14/1.89	396.75/1.85	390.28/1.82	392.30/2.02
225-270	389.13/1.88	394.81/1.86	390.26/1.82	384.40/1.94
270-315	388.68/1.87	398.68/1.89	389.58/1.82	384.99/1.93
315-360	390.87/1.91	401.17/1.89	387.58/1.83	389.32/1.98

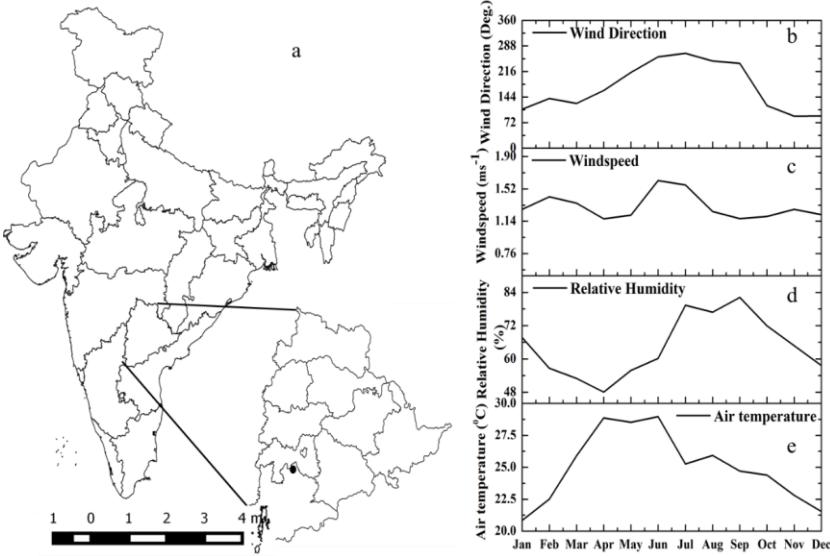
**Table 3** Statistical correlation between CO<sub>2</sub> and CH<sub>4</sub>

1093  
1094  
1095  
1096  
1097  
1098  
1099  
1100  
1101  
1102  
1103  
1104  
1105  
1106  
1107  
1108  
1109  
1110  
1111  
1112  
1113  
1114  
1115  
1116  
1117  
1118  
1119  
1120

S.No	Seasons	Correlation coefficient (R <sup>2</sup> )	Slope $\left(\frac{y_{CH4}(ppm)}{x_{CO2}(ppm)}\right)$	$\Psi_{slope}$ (ppm)	$\Psi_{\gamma-int}$ (ppm)
1	Monsoon (JJAS)	0.6137	0.005	0.00015	1.91
2	Post- monsoon (OND)	0.7252	0.0065	0.00014	1.52
3	Winter (JF)	0.8061	0.0085	0.00018	9.13
4	Pre- monsoon (MAM)	0.8064	0.0059	0.00021	2.73

**Table 4** Cluster analysis of air mass trajectories reaching Shadnagar at various heights during different seasons

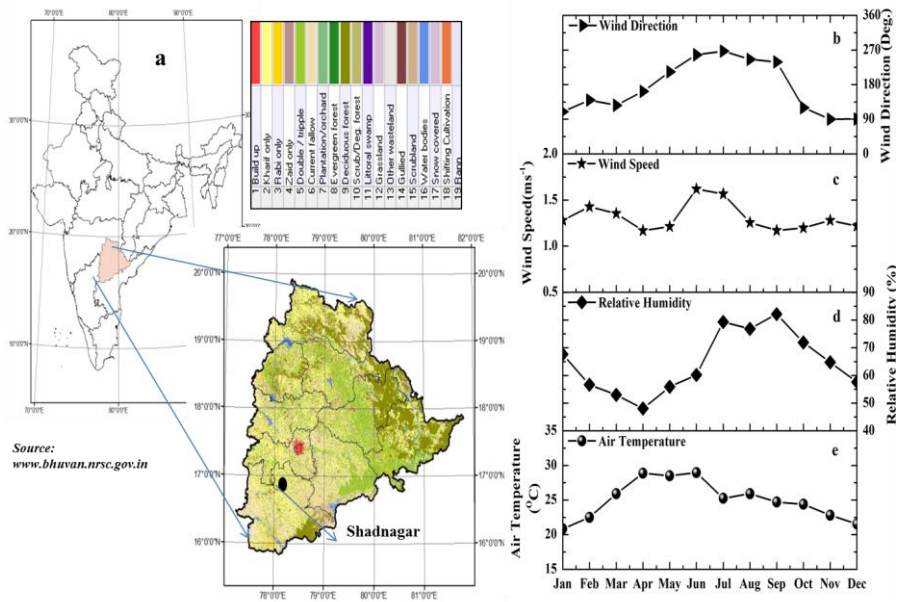
Seasonal Backward trajectory (%)	NW				NE				SE				SW			
	1 km	2 km	3 km	4 km	1 km	2 km	3 km	4 km	1 km	2 km	3 km	4 km	1 km	2 km	3 km	4 km
Winter	54	32	2	0	32	24	44	52	10	25	11	7	4	19	42	41
Pre-monsoon	24	9	8	1	26	31	64	78	36	46	2	10	14	14	26	11
Monsoon	0	1	7	19	12	34	80	70	4	4	4	6	84	61	9	5
Post-monsoon	42	15	11	14	47	53	41	49	8	30	32	26	3	2	16	11



Formatted: Font: (Default) Times New Roman, 12 pt

1143  
1144

Formatted: Font: (Default) Times New Roman, Bold

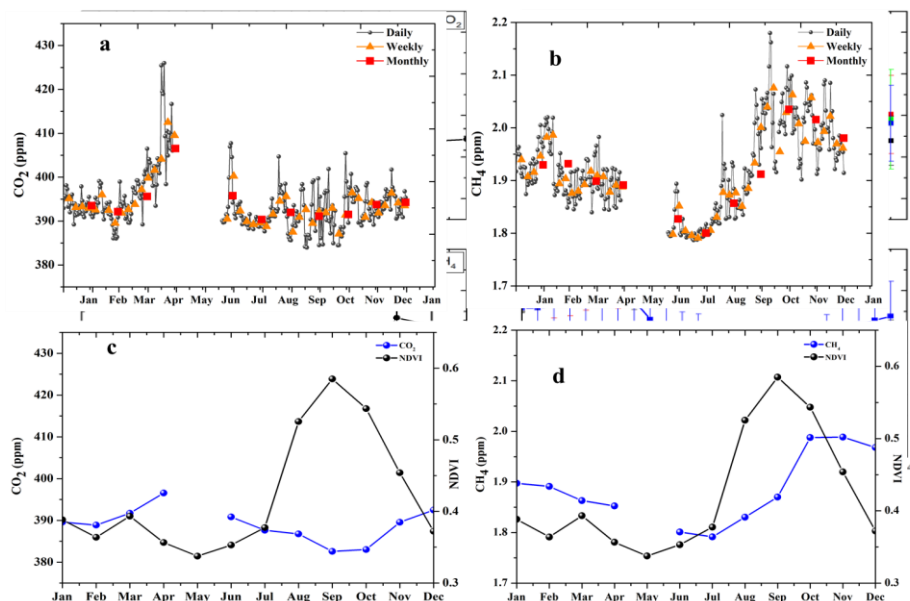


1145  
1146  
1147  
1148  
1149  
1150

**Figure 1** a) Schematic representation of study area; b-e) Seasonal variation of prevailing meteorological conditions during 2014 study period

1151

Formatted: Font: (Default) Times New Roman, Bold



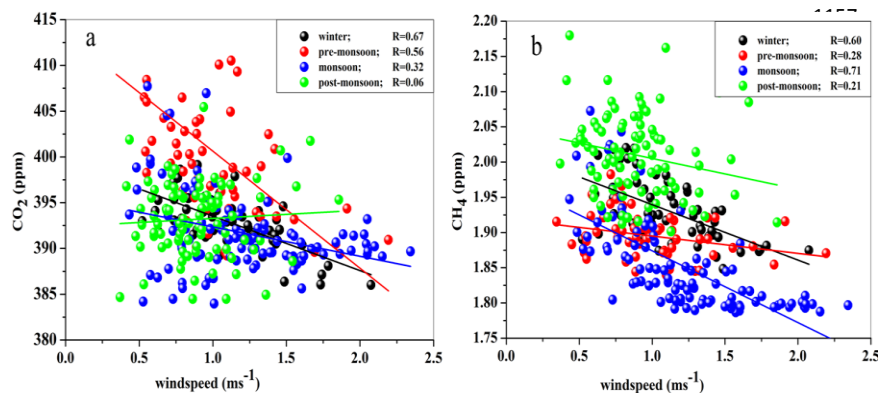
1152

Formatted: Font: (Default) Times New Roman, Bold

1153 **Figure 2** a-b) Temporal Seasonal variations of CO<sub>2</sub> and CH<sub>4</sub>; c-d) Seasonal variations of CO<sub>2</sub> and CH<sub>4</sub> in  
1154 conjunction with NDVI (Normalized Difference Vegetation Index) diurnal variations of CO<sub>2</sub> and CH<sub>4</sub>  
1155 during 2014

Formatted: Subscript

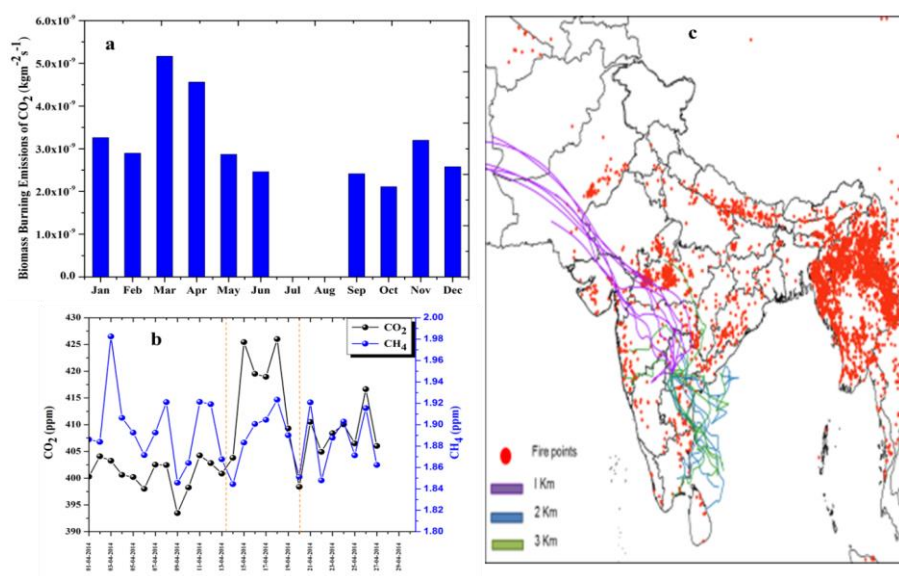
1156



1166



1167  
1168



1169

1170  
1171

1172 **Figure 3** a) Long term analysis of CO<sub>2</sub> biomass burning emissions over study region b) Biomass  
1173 signatures on CO<sub>2</sub>/CH<sub>4</sub> during 14-21 April 2014, a case study c) Spatial distribution of MODIS derived fire  
1174 counts over Indian region during 14-21 April 2014. Scatterplot between wind speed and GHG's (CO<sub>2</sub> and  
1175 CH<sub>4</sub>).

Formatted: Font: (Default) Times New Roman, Bold

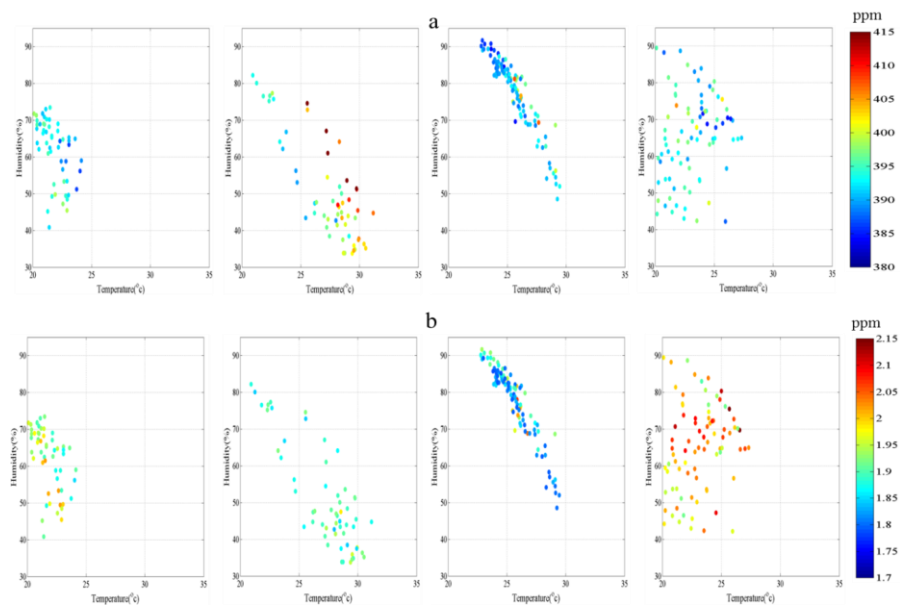
Formatted: Subscript

Formatted: Subscript

Formatted: Font: 11 pt

1176

Formatted: Font: (Default) Times New Roman



1177

1178

1179

1180

1181

1182

1183

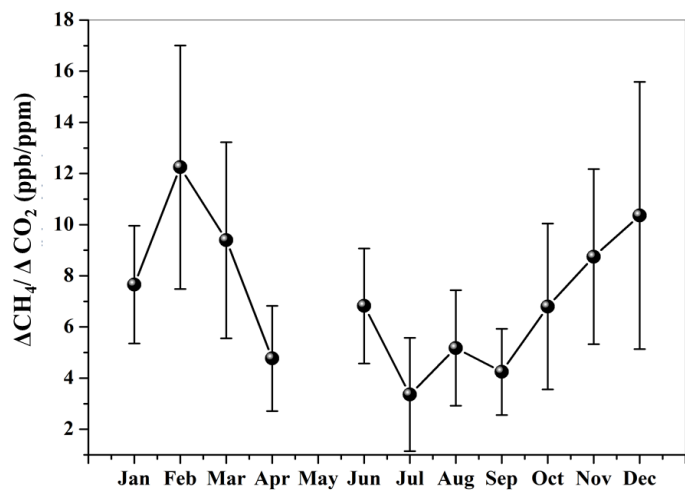
1184

1185

1186

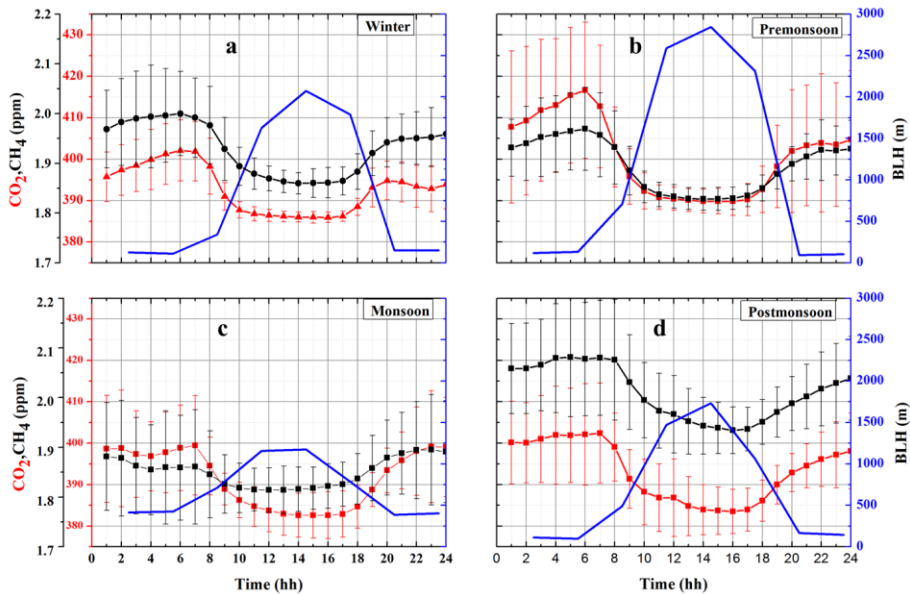
1187

1188



1189 **Figure 4** Monthly variation of  $\Delta\text{CH}_4/\Delta\text{CO}_2$  during study period

Formatted: Font: (Default) Times New Roman

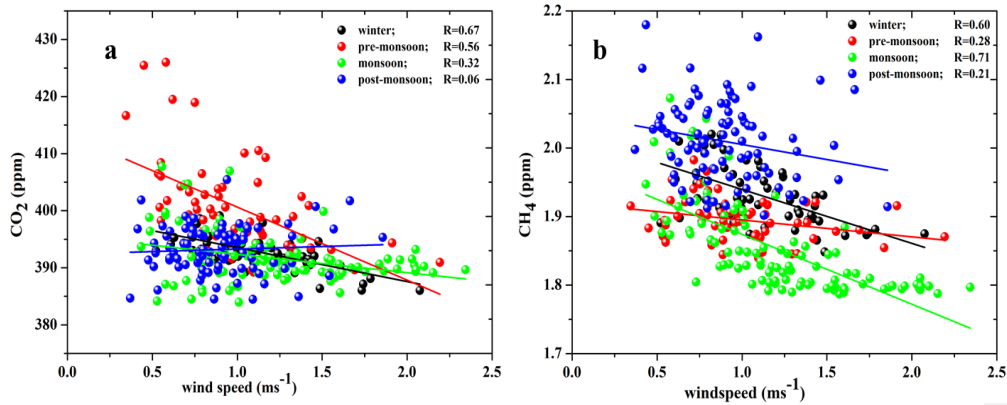


1190 **Figure 5 a-d)** Seasonal variations of diurnal averaged  $\text{CO}_2/\text{CH}_4$  against boundary layer height during 2014

Formatted: Subscript

Formatted: Subscript

Formatted: Font: (Default) Times New Roman

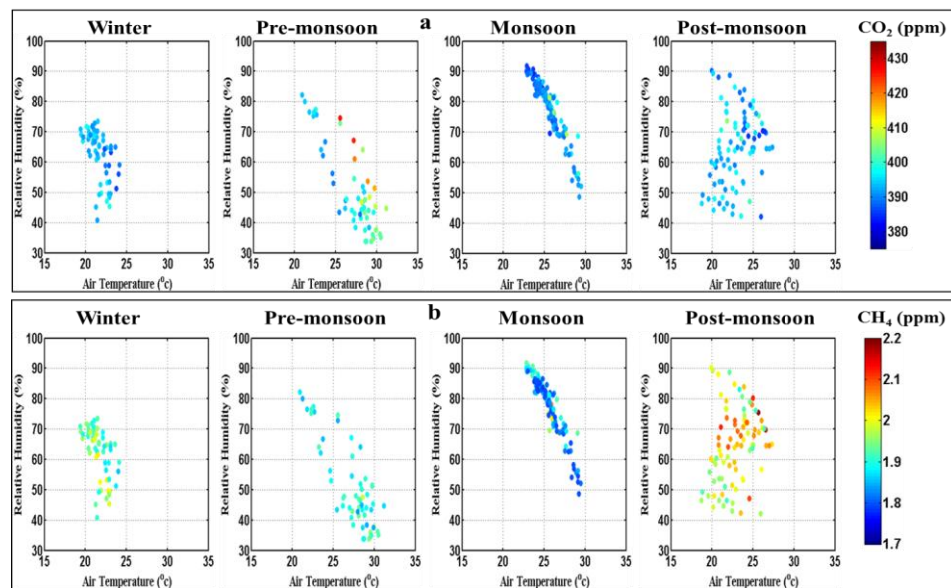


Formatted: Left

1194

Figure 6 a-b) Daily mean scatterplot between wind speed and GHGs ( $\text{CO}_2$  and  $\text{CH}_4$ ).

Formatted: Font: (Default) Times New Roman



1195

Figure 7 a-b) Daily mean seasonal variation of  $\text{CO}_2$  and  $\text{CH}_4$  as function of humidity and air temperature during 2014

Formatted: Subscript

1196

1197

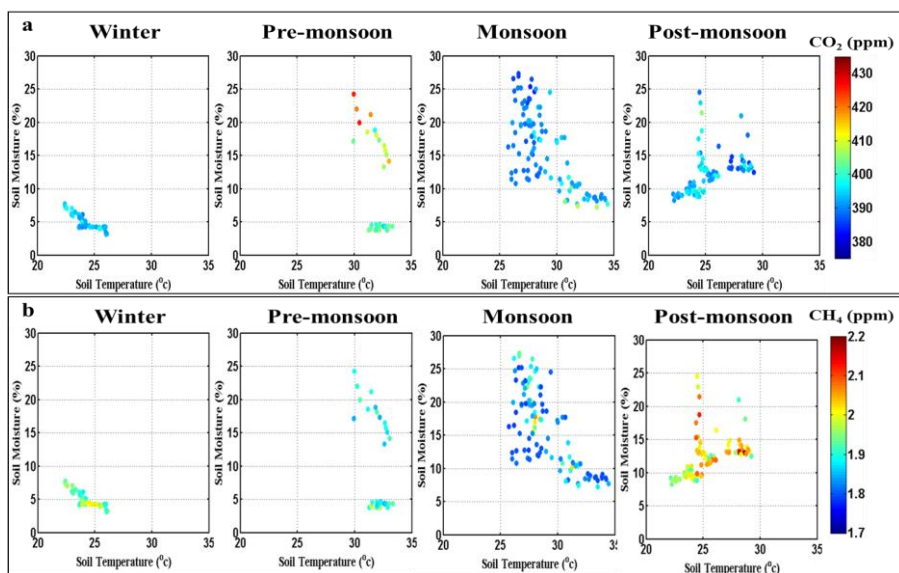
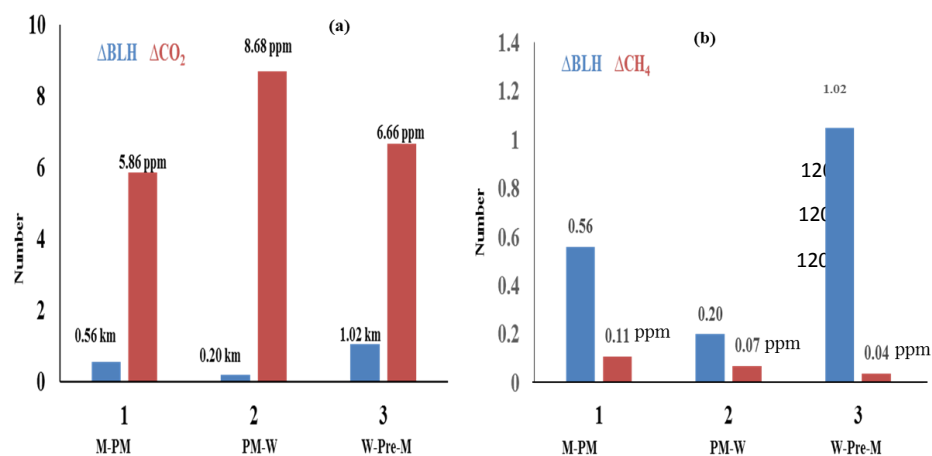
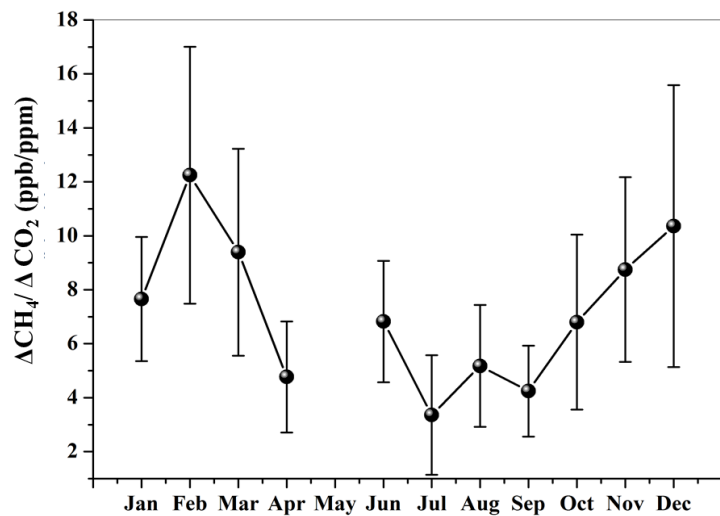


Figure 8 a-b) Daily mean seasonal variation of CO<sub>2</sub> and CH<sub>4</sub> as function of soil temperature and soil moisture during 2014 a) Seasonal variation of CO<sub>2</sub> as function of humidity and temperature during winter, pre-monsoon, monsoon and post-monsoon. b) Seasonal variation of CH<sub>4</sub> as function of humidity and temperature during respective seasons

Formatted: Font: (Default) Times New Roman

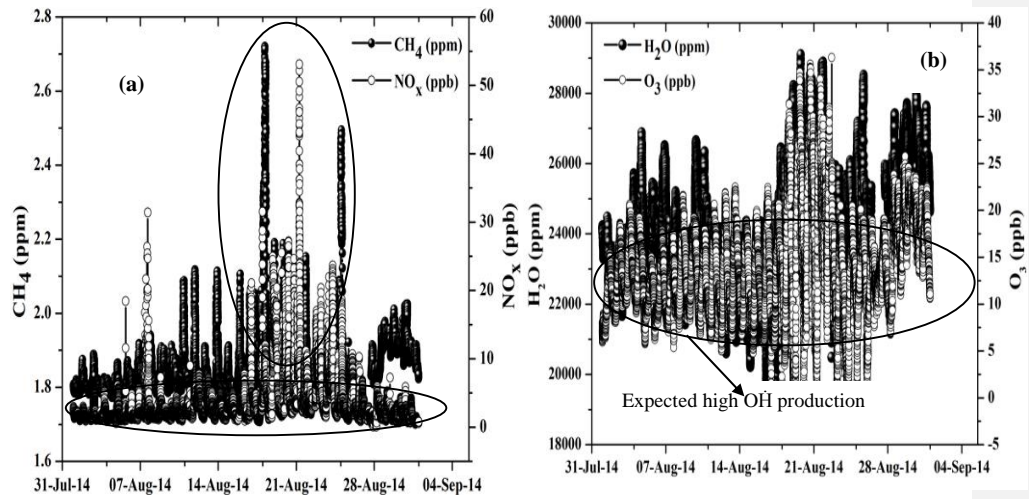


**Figure 59** Seasonal difference in BLH variations of against respective change in -a) CO<sub>2</sub> and b) CH<sub>4</sub> against boundary layer height change



**Figure 6** Monthly variation of ΔCH<sub>4</sub>/ΔCO<sub>2</sub> during study period

1229



1230

1231

1232

1233 **Figure 7** Time series analysis of a) CH<sub>4</sub> vs. NO<sub>x</sub>, b) H<sub>2</sub>O vs. O<sub>3</sub>

1234

1235

1236

1237

1238

1239

1240

1241

1242

1243

1244

1245

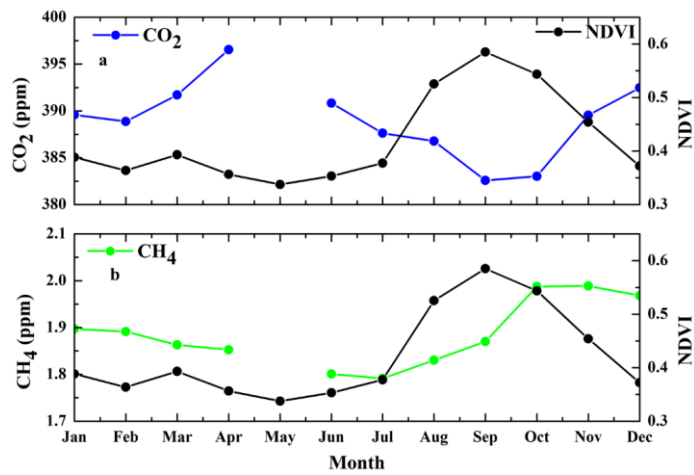


**Figure 8** a) Seasonal variation of CO<sub>2</sub> in conjunction with NDVI (Normalized Difference Vegetation Index). b) Seasonal variation of CH<sub>4</sub> in conjunction with NDVI

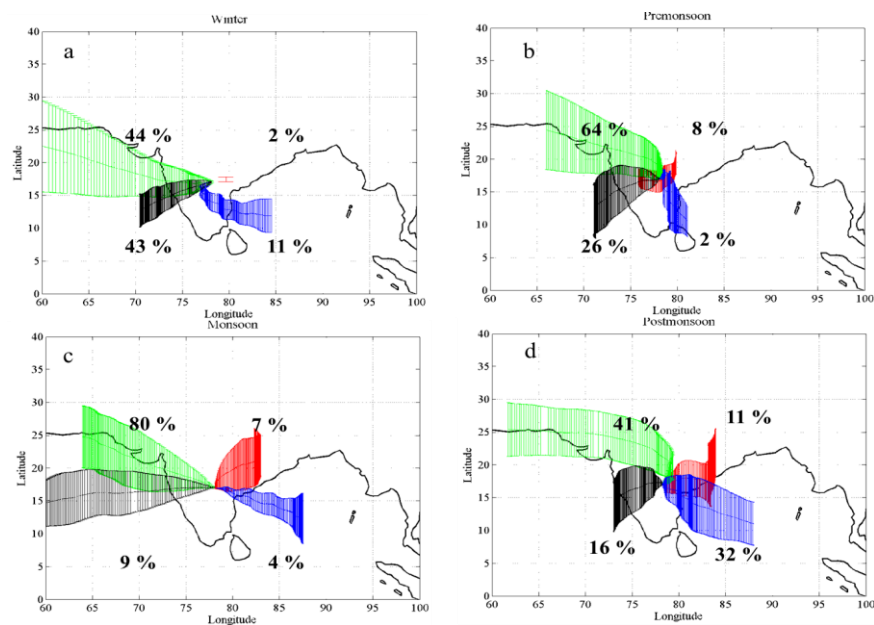


**Figure 9** a-d) Long range circulation of air mass trajectories ending over Shadnagar at 3 km during winter, pre-monsoon, monsoon and post-monsoon



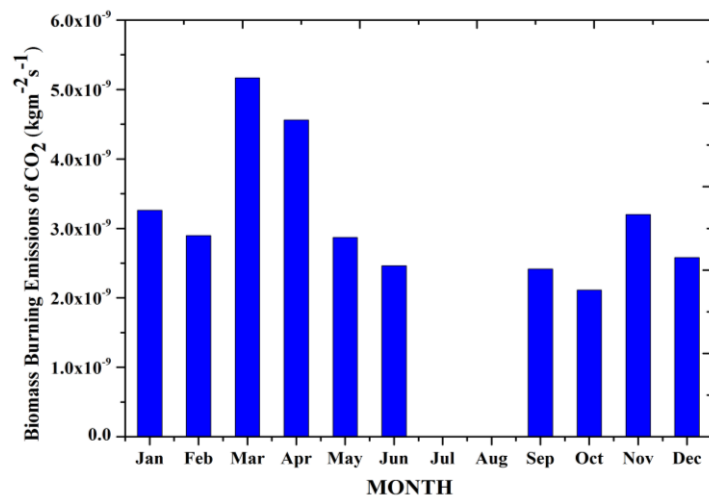


**Figure 10** Long term analysis of CO<sub>2</sub> biomass burning emissions over study region